Measurement of the $t\bar{t}$ production cross section in the dilepton channel in pp collisions at $\sqrt{s} = 7$ TeV

The CMS collaboration

E-mail: cms-publication-committee-chair@cern.ch

ABSTRACT: The $t\bar{t}$ production cross section ($\sigma_{t\bar{t}}$) is measured in proton-proton collisions at $\sqrt{s} = 7$ TeV in data collected by the CMS experiment, corresponding to an integrated luminosity of $2.3\,\text{fb}^{-1}$. The measurement is performed in events with two leptons (electrons or muons) in the final state, at least two jets identified as jets originating from b quarks, and the presence of an imbalance in transverse momentum. The measured value of $\sigma_{t\bar{t}}$ for a top-quark mass of 172.5 GeV is $161.9 \pm 2.5\,(\text{stat.})\,^{+5.1}_{-5.0}\,(\text{syst.}) \pm 3.6\,(\text{lumi.})$ pb, consistent with the prediction of the standard model.

Contents

1   Introduction

A precise measurement of the $t\bar{t}$ production cross section ($\sigma_{t\bar{t}}$) in pp collisions at the Large Hadron Collider (LHC) is important for several reasons. At LHC energies, $t\bar{t}$ production is dominated by gluon-gluon fusion, representing a benchmark for other processes of the standard model (SM) initiated through the same mechanism, such as the production of Higgs bosons. In addition, a precise value of $\sigma_{t\bar{t}}$ can provide constraints on parton distribution functions (PDF) and be used to check the validity of perturbative calculations in quantum chromodynamics (QCD). It can also benefit searches for physics beyond the SM, as $t\bar{t}$ production is often a major source of background.

The precision of initial measurements of $\sigma_{t\bar{t}}$ in 2010 at $\sqrt{s} = 7$ TeV [1, 2] has been improved in refs. [3–8], and measurements of electroweak single-top-quark production are available in refs. [9, 10]. By now, many top-quark events have been collected at the LHC, with studies proceeding on a variety of top-quark production and decay channels [5, 11–13], as well as on searches for deviations relative to predictions of the SM.

This work presents a measurement of $\sigma_{t\bar{t}}$ in dilepton final states that improves upon a previous measurement [5] of the Compact Muon Solenoid (CMS) experiment [14]. It is based on more refined event selections and analysis techniques, an improved estimation of systematic uncertainties, and with a data sample approximately sixty times larger. Starting from the nearly 100% decay of both top quarks through the electroweak transition $t \to Wb$, we focus on events in the dilepton final states e^+e^-, $\mu^+\mu^-$, and $e^\pm\mu^\mp$, where both W bosons decay leptonically ($W \to \ell\nu_\ell$), but with contributions from $W \to \tau\nu_\tau$ arising only when the τ leptons decay into $\ell\nu_\ell\nu_\tau$ (ℓ = e or μ) states. A cross-section measurement based on τ leptons that decay into hadrons and a neutrino can be found in ref. [15]. The final states contain two leptons of opposite electric charge, their accompanying neutrinos from the W-boson decays, and two jets of particles resulting from the hadronization of the b quarks. These modes correspond to $(6.45 \pm 0.11)\%$ [16] of all $t\bar{t}$ decay channels, including the partial contributions from τ leptons.

This measurement is based on a data sample corresponding to an integrated luminosity of $2.3 \pm 0.1\,\text{fb}^{-1}$ recorded by the CMS experiment. A profile likelihood-ratio (PLR) method [17, 18], as well as a counting analysis based on direct selections, are used to extract the $t\bar{t}$ cross section.

A brief description of the components of the CMS detector specific to this analysis is provided in section 2, followed by details of event Monte Carlo (MC) simulation in section 3, and event selection in section 4. Estimations of backgrounds yields are presented in section 5. Following a discussion of systematic uncertainties in section 6, the event yields in data are compared with simulations in section 7. The results of the measurement of the $t\bar{t}$ cross section are presented in section 8, followed by a summary in section 9.

2   The CMS detector

The central feature of the CMS apparatus is a superconducting solenoid, 13 m in length and 6 m in diameter, which provides an axial magnetic field of 3.8 T. The bore of the solenoid is outfitted with a variety of particle-detection systems. Charged-particle trajectories are measured with the silicon pixel and strip trackers that cover $0 < \phi < 2\pi$ in azimuth and $|\eta| < 2.5$ in pseudorapidity, where η is defined as $\eta = -\ln[\tan(\theta/2)]$, with θ being the polar angle of the trajectory of the particle with respect to the anticlockwise beam direction. A crystal electromagnetic calorimeter (ECAL) and a brass/scintillator hadronic calorimeter surround the inner tracking volume and provide high-resolution measurements of energy (E) used to reconstruct electrons, photons and particle jets. Muons are measured in gas detectors embedded in the flux-return yoke of the solenoid. The detector is nearly hermetic, thereby providing reliable measurements of momentum imbalance in the plane transverse to the beams. A two-tier trigger system selects the most interesting pp collisions for analysis. A more detailed description of the CMS detector is given in ref. [14].

3 Simulation of signal and backgrounds

The $t\bar{t}$ cross section, calculated with the MCFM program [19, 20] at next-to-leading order (NLO) in perturbative QCD, assuming a top-quark mass of $m_t = 172.5\,\text{GeV}$, is $158^{+23}_{-24}\,\text{pb}$. Several approximate next-to-next-to-leading-order (NNLO) calculations are also available in the literature, in particular those of Kidonakis ($163\,^{+11}_{-10}\,\text{pb}$ [21]), Ahrens et al. ($149 \pm 11\,\text{pb}$ [22]) and the HATHOR program ($164\,^{+13}_{-10}\,\text{pb}$ [23]), with the latter used to normalize the distributions and yields of simulated $t\bar{t}$ events to the measured luminosity. However, this cross section is used just to present expected rates in figures and tables and has no effect on the final measurement.

Signal and background events are simulated using the MC event generators MAD-GRAPH (v. 5.1.1.0) [24], POWHEG (r1380) [25] or PYTHIA (v. 6.424) [26], depending on the process in question. MADGRAPH is used to model $t\bar{t}$ events, with matrix elements corresponding to up to three additional partons that are matched to PYTHIA, which is used for the subsequent hadronization. Decays of τ leptons are handled with TAUOLA (v. 2.75) [27].

MADGRAPH is also used to simulate the W+jets and Drell-Yan (DY: $q\bar{q} \to Z/\gamma^\star$+jets, where $\gamma^\star$ represents the contribution from virtual photons) background samples, with up to 4 partons in the final state. For W+jets, the MADGRAPH sample provides only event with leptonic decays of W bosons. The total inclusive NNLO cross section of $31.3 \pm 1.6\,\text{nb}$ is calculated with the FEWZ program [28]. Simulations of DY events with two oppositely charged leptons of same flavor in the final state are generated for dilepton invariant masses between 10 and $50\,\text{GeV}$, as well as for $>50\,\text{GeV}$. The corresponding NNLO cross sections, also calculated with FEWZ are $11.91 \pm 0.64\,\text{nb}$ and $3.04 \pm 0.13\,\text{nb}$, respectively. Single-top-quark events ($pp \to tW^-$ and $pp \to \bar{t}W^+$) are simulated in POWHEG, for a cross section of $15.7 \pm 0.4\,\text{pb}$ (calculated at approximate NNLO [29]). Inclusive production of the WW, WZ, and ZZ diboson final states is simulated with PYTHIA, and the respective cross sections are $47.0 \pm 1.5\,\text{pb}$, $18.2 \pm 0.7\,\text{pb}$, and $7.7 \pm 0.2\,\text{pb}$.

Among all of the simulated backgrounds, only the contributions from WW, WZ, and ZZ (referred as diboson in the text and labeled as VV in figures) and single-top-quark production are used to estimate the absolute number of background events. Recent measurements of single-top-quark and diboson cross sections show good agreement with SM predictions [8, 9, 30–33]. All other backgrounds are estimated from control samples in data.

Effects from additional pp interactions (pileup) are modeled by adding simulated minimum-bias events (generated with PYTHIA) to the simulated processes, using a pileup multiplicity distribution that reflects the luminosity profile of the observed pp collisions. The CMS detector response is simulated using GEANT4 (v. 9.4) [34].

4 Event selection

Events are collected using dilepton triggers (excluding "hadronic" τ triggers) that require the presence of two large transverse momentum (p_T) leptons. The definitions and ranges of thresholds, isolation and identification requirements for dilepton triggers were changed periodically during data taking so as to adapt to changes in instantaneous luminosity

delivered by the LHC. In particular, electrons selected at the trigger stage must pass a threshold on electron transverse energy E_T, that ranges from 8 to 17 GeV, as measured online by combining information from ECAL with that from the inner tracker, and muons identified in muon detectors are similarly required to exceed a threshold on p_T, that ranges between 7 and 17 GeV as measured online by combining information from the outer muon detector with that from the inner tracker.

The efficiency for $t\bar{t}$ dilepton triggers is measured in data through other triggers that are only weakly correlated with the dilepton-trigger requirements. Because of the presence of a significant imbalance in transverse momentum in $t\bar{t}$ events, $\not{E}_T$-based triggers with different $\not{E}_T$ thresholds are used for this purpose. At the trigger level, the $\not{E}_T$ is defined by the magnitude of the vector $\vec{\not{E}}_T = -\sum \vec{E}_T$, using the transverse energies of calorimeter towers. Studies based on simulated events indicate that the $\not{E}_T$ triggers are uncorrelated with the dilepton triggers.

Using the measured dilepton-trigger efficiency in data, the corresponding efficiencies in simulations are corrected by multiplicative data-to-simulation scale factors (SF) of 0.962 ± 0.015, 0.977 ± 0.016, and 1.008 ± 0.009 for the e^+e^-, $\mu^+\mu^-$ and $e^\pm\mu^\mp$ final states, respectively, to provide agreement between data and simulation.

The first step in the offline selections requires the presence of a proton-proton interaction vertex [35] within 24 cm of the detector center along the beam line direction, and within 2 cm of the beam line in the transverse plan. These selections have an efficiency >99.5% for events with two leptons that pass selection criteria. The main primary vertex of an event corresponds to the vertex with the largest value for the scalar sum of the transverse momenta of the associated tracks.

At least two leptons in the event (either electrons or muons) are required to pass identification and isolation requirements. The selection criteria are similar to those of refs. [1, 5], and can be described briefly as follows. Electron candidates [36] are based on a cluster of energy depositions in the ECAL. Clusters are matched to hits in the silicon tracker using a track reconstruction algorithm that takes into account possible energy loss due to bremsstrahlung. Muon candidates are reconstructed by combining information from the inner tracker with information from the outer muon detectors [37].

Both leptons must have $p_T > 20$ GeV, with electrons and muons being restricted to $|\eta| < 2.5$ and $|\eta| < 2.1$, respectively. The lepton-candidate tracks are required to be consistent with originating from the primary vertex, and must satisfy additional quality requirements, as described in refs. [1, 5]. Lepton candidates are required to be isolated from other energy depositions in the event. A cone of $\Delta R = \sqrt{(\Delta\eta)^2 + (\Delta\phi)^2} < 0.3$, where $\Delta\eta$ and $\Delta\phi$ are the differences in pseudorapidity and azimuthal angle between any element of energy and the axis of the lepton, is constructed around the initial direction of the candidate. The particle energies within this cone, obtained using the particle-flow (PF) reconstruction algorithm [38], which provides a list of particles and their kinematic properties, are projected onto the plane transverse to the beam, and summed as scalar quantities, excluding the contribution from the lepton candidate. In this procedure, all charged PF particles not associated with the main primary vertex are assumed to arise from pileup events, and are excluded from the sum. Then, the relative isolation discriminant, I_{rel},

is defined as the ratio of this sum to the transverse momentum of the lepton candidate. A lepton candidate is not considered as isolated and is rejected if the value of I_{rel} is >0.20 for a muon and >0.17 for an electron. These selections are optimized using simulated $t\bar{t}$ events.

The efficiency of lepton selection is measured using a "tag-and-probe" method in dilepton events enriched in Z-boson candidates, and indicates that electron and muon reconstruction efficiencies are >99% [39]. The efficiencies for the above lepton-identification requirements, calculated as function of the p_{T} and η of the leptons, are in the range of 98–99% for muons and 85–94% for electrons. The average efficiency of the lepton-isolation criterion measured in such Z events is in the range of 90–99% for both muons and electrons. The efficiencies measured in data are found to be very close to the estimates from the DY simulation. Based on an overall comparison of lepton-selection efficiencies in data and simulations, the event yield in simulation is corrected by multiplicative scale factors of 0.995 ± 0.003, 0.997 ± 0.005 and 0.994 ± 0.005 for the $\mathrm{e^+e^-}$, $\mu^+\mu^-$ and $\mathrm{e^\pm\mu^\mp}$ final states, respectively, to provide consistency with data.

Accepted events are required to have at least one pair of oppositely charged leptons. While muon-charge misidentification is negligibly small, the electron-charge misidentification rate is 0.8%, as measured from $\mathrm{Z} \rightarrow \mathrm{e^+e^-}$ decays. Dilepton $t\bar{t}$-candidate events with invariant mass $M_{\ell\ell} < 20\,\mathrm{GeV}$ are removed from all three channels, with a consequent reduction of about 2% in $t\bar{t}$ signal. However, this requirement significantly suppresses backgrounds from heavy-flavor resonances, as well as contributions from low-mass DY processes. In events containing several possible $\ell^+\ell^-$ pairs that pass all acceptance requirements, only the pair of leptons with the highest sum of scalar transverse momenta is retained. To suppress contributions from Z boson production, the invariant mass of the dilepton system is required to be outside the range of 76 to 106 GeV for both the $\mathrm{e^+e^-}$ and $\mu^+\mu^-$ modes. According to simulation, this invariant mass requirement rejects about 91% of the DY events, at the cost of rejecting ≈24% of both the $\mathrm{e^+e^-}$ and $\mu^+\mu^-$ $t\bar{t}$ signal events.

The anti-k_{T} clustering algorithm [40] with a distance parameter $R = 0.5$ is used for jet clustering. Jets are reconstructed based on information from the calorimeter, tracker, and muon systems [41] using PF reconstruction. Jet energy corrections rely on simulations and on studies performed with exclusive two-jet and photon+jet events in data. To minimize the impact of pileup, charged PF particles not associated with the primary event vertex [38] are ignored in reconstructing jets. After eliminating the charged component of pileup events, the neutral component is removed by applying a residual energy correction, following the "area-based" procedure described in refs. [42, 43]. Jets are also required to satisfy $p_{\mathrm{T}} > 30\,\mathrm{GeV}$ and $|\eta| < 2.5$. For dilepton $t\bar{t}$ candidates with at least two jets and before applying any b-tagging requirement, both b-quark jets from $t\bar{t}$ decays pass the jet selection criteria in about 65% of the events, as predicted by the $t\bar{t}$ simulation.

For the offline analysis, the missing transverse energy ($E\!\!\!/_{\mathrm{T}}$) is redefined by the magnitude of the vectorial sum of the particle transverse momenta $\vec{E\!\!\!/}_{\mathrm{T}} = -\sum \vec{p}_{\mathrm{T}}$, calculated using the particles reconstructed with the PF algorithm [44]. As implied above, $E\!\!\!/_{\mathrm{T}}$ corresponds to a distinguishing feature of $t\bar{t}$ events in the dilepton channel because of escaping energetic neutrinos. Neither the dominant DY background ($\mathrm{Z}/\gamma^\star \rightarrow \mathrm{e^+e^-}$ and $\mu^+\mu^-$), nor the smaller background from false isolated leptons in multijet events, provide a source of

large $E\!\!\!/_T$. We require $E\!\!\!/_T > 40\,\mathrm{GeV}$ in the $\mathrm{e^+e^-}$ and $\mu^+\mu^-$ modes in $\mathrm{t\bar{t}}$ events with at least two jets. This cut causes a loss of $\approx 25\%$ of $\mathrm{t\bar{t}}$ signal in these channels, but reduces the contribution from DY production by about a factor of 30. No $E\!\!\!/_T$ requirement is imposed for the $\mathrm{e^\pm\mu^\mp}$ mode, as there is very little contamination from DY events in this channel.

To account for any mismodeling of the $E\!\!\!/_T$ distribution, the efficiency of the $E\!\!\!/_T$ selection in the $\mathrm{t\bar{t}}$ simulation is corrected using data. The corresponding data-to-simulation SF are estimated by applying the $E\!\!\!/_T$ selection to $\mathrm{e^\pm\mu^\mp}$ data, after correcting for the presence of background. The systematic uncertainties on these factors arise from two sources: (i) the background contamination in the $\mathrm{e^\pm\mu^\mp}$ channel, which is changed in the study by $\pm\,30\%$, and (ii) the difference in lepton energy resolution between electrons and muons, which affects differently the $E\!\!\!/_T$ in $\mathrm{e^+e^-}$ and $\mu^+\mu^-$ channels relative to the $\mathrm{e^\pm\mu^\mp}$ channel. The data-to-simulation SF are 1.008 ± 0.012 and 1.008 ± 0.016 for the $\mathrm{e^+e^-}$ and $\mu^+\mu^-$ final states, respectively, with the uncertainties accounting for both statistical and systematic effects summed in quadrature.

As dilepton $\mathrm{t\bar{t}}$ events contain jets from the hadronization of b quarks, requiring b tagging can reduce background from events that do not contains b jets. Jets are identified as b jets originating from b quarks through a "combined secondary vertex" (CSV) algorithm [45], which provides a b-tagging discriminant by combining information from secondary vertices and track-based lifetime measurements. The chosen b-tagging selection has an efficiency of 80–85% for each b jet in dilepton $\mathrm{t\bar{t}}$ events, and a 10% mistagging rate for light-flavor or gluon jets misidentified as b jets, both estimated from inclusive simulated $\mathrm{t\bar{t}}$ events. The b-tagging efficiency can be estimated from $\mathrm{t\bar{t}}$ events in data, as described in ref. [46]. To avoid statistical correlations between the extraction of the b-tagging efficiency and the $\mathrm{t\bar{t}}$ cross section, the b-tagging performance is measured from multijet events in data [45], and used to correct the b-tagging performance of the simulation. This analysis uses the b-tagging information either as input to a likelihood fit (in the PLR method presented in section 8.1) or directly to select events that are required to contain at least one b-tagged jet (in a counting analysis used as a cross-check, and presented in section 8.2).

5   Background estimates

The main backgrounds in this analysis arise from DY, diboson, and single-top-quark events (tW), where at least two prompt leptons are produced from Z or W decays. Other background sources, such as $\mathrm{t\bar{t}}$ events with decays to lepton+jets or no leptons at all (all jets), or generic multijet (MJ) events, are related to the presence of at least one jet reconstructed incorrectly as a lepton, which mainly happens for electrons, or a lepton from the decay of bottom or charm hadrons, which mainly happens for muons.

The yields from background processes with smallest contributions to $\mathrm{t\bar{t}}$ candidates, corresponding to single-top-quark and diboson production, are estimated directly from simulations. This section focuses on other backgrounds, which are not adequately described through simulation, such as the DY contribution, and events with leptons that do not arise from W or Z decays. In these cases, the background estimates are based on data.

5.1 Backgrounds from Drell-Yan contribution

To estimate the background from DY events contributing into e^+e^- and $\mu^+\mu^-$ $t\bar{t}$ final states, we use the method described in refs. [1, 5]. The number of DY events in data that pass the Z-boson veto on $M_{\ell\ell}$ can be estimated from the number of events in data with a dilepton invariant mass within $76 < M_{\ell\ell} < 106\,\mathrm{GeV}$, scaled by the ratio ($R_{\mathrm{out/in}}$) of events that fail and that pass this selection, which is estimated through DY simulation.

To achieve a better estimate of this background, the value of $R_{\mathrm{out/in}}$ is corrected using data. In particular, $R_{\mathrm{out/in}}$ is sensitive to detector effects, such as the modeling of lepton resolution and the dependence of the fraction of vetoed DY events for different requirements on jet multiplicities. The value of $R_{\mathrm{out/in}}$ is corrected for these effects by using control regions enriched in DY events in data.

A 15% systematic uncertainty is assigned to account for remaining discrepancies in the dependence of $R_{\mathrm{out/in}}$ on $\not{E}_{\mathrm{T}}$. Using the data-corrected $R_{\mathrm{out/in}}$ values leads to the final data-to-simulation scale factors of 1.86 ± 0.50 and 1.76 ± 0.36 for the e^+e^- and $\mu^+\mu^-$ channels, respectively. After requiring at least one b-tagged jet, there are too few events in data to perform a precise estimation, which leads to larger uncertainties on the corresponding scale factors, yielding 2.04 ± 0.52 and 1.67 ± 0.42 for the e^+e^- and $\mu^+\mu^-$ channels, respectively.

Finally, most of the background contribution in the $e^\pm\mu^\mp$ channel is from $Z/\gamma^* \to \tau\tau \to e\nu_e\nu_\tau\mu\nu_\mu\nu_\tau$ events. As the yield from this final state corresponds to a fraction of about 3% of the total DY cross section, its impact is expected to be small. In addition, because of the presence of additional neutrinos from τ decays, the dilepton invariant mass is often well below the value of the Z-boson mass. The DY contamination of the $e^\pm\mu^\mp$ channel is therefore estimated through a fit of two components to the dilepton invariant-mass distribution, one component reflecting the dilepton mass distribution for $Z/\gamma^\star$ events, and the other corresponding mainly to $t\bar{t}$, single-top-quark and diboson events. The templates for these components are extracted from simulations. The systematic effects that arise from the small contamination of single-top-quark and diboson events are negligible relative to the large statistical uncertainty of the fit. The data-to-simulation scale factor for the $e^\pm\mu^\mp$ channel, following the jet selection, is found to be 1.34 ± 0.29.

The estimates of the DY contributions to the $t\bar{t}$ data sample are given in section 7, before and after requiring at least one b-tagged jet.

5.2 Backgrounds with leptons not from W/Z decays

A data-based method is also used to estimate the background from misidentified leptons, and from well-identified leptons that pass the isolation requirement but which come from semi-leptonic decays of bottom or charm hadrons contained within jets. These leptons are referred to as non-prompt leptons in the following. Three categories of backgrounds can be defined: signal-like, W-like, and MJ-like sources, containing two, one, and no true isolated (prompt) leptons, respectively. The signal-like sample contains $t\bar{t}$ signal events, but also DY, single-top-quark, and diboson events. The W-like sample consists of W+jets events and $t\bar{t}$ events observed in the lepton+jets channel. The MJ-like sample contains mainly generic multijet events or $t\bar{t}$ events in all-jets final states.

	Before b tagging			Requiring ≥ 1 b-tagged jet		
	e^+e^-	$\mu^+\mu^-$	$e^\pm\mu^\mp$	e^+e^-	$\mu^+\mu^-$	$e^\pm\mu^\mp$
N_{W}	7.8 ± 5.9	14.9 ± 7.1	63.8 ± 16.8	1.8 ± 4.8	9.8 ± 5.6	42.4 ± 14.6
N_{MJ}	0.7 ± 0.6	0.4 ± 0.3	21.1 ± 10.0	0.6 ± 0.5	0.2 ± 0.1	7.5 ± 3.9

Table 1. Estimated number of W-like (N_{W}) and MJ-like (N_{MJ}) background events in data before and after b tagging.

The number of events in each of the above categories is defined by relaxing the single-lepton isolation from $I_{\mathrm{rel}} < 0.17$ and $I_{\mathrm{rel}} < 0.20$ for electrons and muons, respectively (which corresponds to the definition of "tight" leptons), to $I_{\mathrm{rel}} < 0.8$ for both flavors of leptons (which defines "loose" leptons). Dilepton samples are then constructed to correspond to loose, medium, and tight events, respectively, defined by two loose, at least one tight, and two tight isolated leptons. Only the tight dilepton sample is used to measure $\sigma_{t\bar{t}}$.

By introducing probabilities for a loose event to pass medium or tight criteria, and the probability of a medium event to be accepted as a tight event, a system of equations can be constructed to estimate the number of signal-like, W-like, and MJ-like events. The probabilities can be expressed in terms of individual probabilities for prompt and non-prompt leptons that pass the relaxed isolation selection to also pass the tight isolation requirement. The prompt-lepton efficiencies are estimated using Z events in data, in a manner similar to that discussed in section 4, while the rates for non-prompt leptons are estimated using a data sample enriched in multijet events. The corresponding systematic uncertainties are estimated by half of the difference between efficiencies determined from data and from simulation studies.

The estimated number of W-like (N_{W}) and MJ-like (N_{MJ}) background events in data before and after requiring at least one b-tagged jet are presented in table 1. The uncertainties account for both statistical and systematic contributions to the efficiency for single prompt and non-prompt loose leptons to pass the tight selection. The effect of the b-tagging selection efficiency and mistagging rates are estimated from simulation.

6   Sources of systematic uncertainty

Systematic uncertainties considered in this measurement include those from biases in detector performance, deviations in $t\bar{t}$-signal acceptance due to ambiguities in modeling $t\bar{t}$ production, precision of background estimates, and the uncertainty on integrated luminosity [47].

A correction is applied to event rates in simulated $t\bar{t}$ samples, to account for differences in dilepton-trigger and dilepton offline selection efficiencies between data and simulations, as described in section 4. The combined data-to-simulation SF, with their uncertainties defined by adding the statistical and systematic sources in quadrature, are $\mathrm{SF^{ee}} = 0.957 \pm 0.016$, $\mathrm{SF^{\mu\mu}} = 0.974 \pm 0.016$, and $\mathrm{SF^{e\mu}} = 1.002 \pm 0.010$, for the e^+e^-, $\mu^+\mu^-$, and $e^\pm\mu^\mp$ $t\bar{t}$ final states, respectively.

Systematic uncertainties arising from the lepton energy scale are estimated by comparing the position of the dilepton invariant-mass peak in $Z/\gamma^\star$-enriched events in data with simulations, applying only trigger and dilepton selection criteria. The effect corresponds to a 0.3% uncertainty on the $t\bar{t}$ selection efficiency for all three dilepton final states.

The uncertainties on jet energy scale (JES) and jet energy resolution (JER) affect the efficiency of jet selection. The impact of uncertainty on JES is estimated from the change observed in the number of selected MC $t\bar{t}$ events after changing the jet momenta within the JES uncertainties [48]. Similarly, the effect of the JER uncertainty is estimated by changing the resolution on jet momenta by $\pm 10\%$, and then estimating the corresponding change in the number of selected MC $t\bar{t}$ events. The systematic uncertainty on $\not{E}_\mathrm{T}$ is discussed in section 4.

After requiring at least one b-tagged jet, the uncertainties on the data-to-simulation factors for b tagging are propagated to the selection efficiency in the simulated $t\bar{t}$ samples. The uncertainties on the b-tagging scale factors in $t\bar{t}$ signal events are $\approx 2\%$ for b jets and $\approx 10\%$ for mistagged jets [45].

The 8% uncertainty in the inelastic proton-proton cross section at $\sqrt{s} = 7\,\mathrm{TeV}$ [49], when propagated to the modeling of pileup, leads to an uncertainty of 0.5% on the yield of simulated $t\bar{t}$ events.

Systematic uncertainties on the MC modeling of $t\bar{t}$ production are estimated by using MadGraph with different parameter settings, such as renormalization/factorization scales μ, which are increased and decreased by a factor of 2 to estimate the effect on the calculated $t\bar{t}$ cross section. Other studies change the threshold that controls the matching of partons from the matrix element with those from parton showers. Systematic uncertainties in the $t\bar{t}$ event selection efficiency from independent changes in the two μ scales and in the matching of partons produce a total uncertainty of 0.6% for each source. Systematic effects from the choice of parton distribution functions are also studied and found to be negligible.

The systematic uncertainty arising from the uncertainty on the measured values of leptonic branching fractions of the W boson (0.1080 ± 0.0009 [16]) translates into a 1.7% uncertainty on the number of selected MC $t\bar{t}$ events. This uncertainty can be reduced through a more precise measurement of the leptonic branching fractions of the W and used to recalculate the measured cross section.

Uncertainties on the selected number of single-top-quark and diboson events are estimated through simulation, and arise from the same kind of sources that affect the $t\bar{t}$ signal. The above-described detector effects contribute to an 8% uncertainty on the number of selected background events, which is dominated by the uncertainty on the JES. In events with at least one b-tagged jet, the uncertainty from b tagging is $\approx 15\%$ for diboson and 5% for single-top-quark events, arising mainly from misidentification of light-flavor jets. In addition, an uncertainty in the cross section for single-top-quark and diboson backgrounds, estimated to be $\approx 20\%$ [9, 31–33], is added in quadrature.

Table 2 summarizes the impact of relative systematic uncertainties from selection efficiencies in simulated $t\bar{t}$ signal events. Uncertainties on background contamination from DY processes and from events with non-prompt leptons are estimated from data, as described in sections 5.1 and 5.2, and given in table 3 of section 7.

	Uncertainty on number of $t\bar{t}$ events (%)	
Source	Without b tagging	$\geq$1 b-tagged jet
Luminosity	2.2	2.2
Lepton efficiencies	1.7 (ee) / 1.7 ($\mu\mu$) / 1.0 (eμ)	1.7 (ee) / 1.7 ($\mu\mu$) / 1.0 (eμ)
Lepton energy scale	0.3	0.3
Jet energy scale	1.8	1.9
Jet energy resolution	0.5	0.3
$\not{E}_{\rm T}$ efficiency	1.4	1.3
b tagging	-	0.7
Pileup	0.5	0.5
Scale of QCD (μ)	0.6	0.6
Matching partons to showers	0.6	0.6
W branching fraction	1.7	1.7

Table 2. Summary of the relative (%) systematic uncertainties on the number of signal $t\bar{t}$ events, after applying the full selection criteria, both, before b tagging and with at least one b-tagged jet in the event. Combined uncertainties are listed for the sum of contributions from the three dilepton channels, except for lepton efficiencies, which are given separately for e^+e^-, $\mu^+\mu^-$, and $e^\pm\mu^\mp$ events.

7 Event yields and distributions

In this section, the predicted distributions from simulation are compared with those from data. When possible, the yields predicted for background are estimated using data, as discussed in section 5. The remaining backgrounds, as well as the distributions in simulated $t\bar{t}$ events, are scaled to the measured integrated luminosity, assuming a $t\bar{t}$ cross section of 164 pb [23]. In the figures below, the hatched regions correspond to uncertainties on the predicted event yields.

Transverse momentum distributions of leptons and jets are shown, respectively, for the largest (leading) $p_{\rm T}$ and next-to-largest (next-to-leading) $p_{\rm T}$ of each set of these objects, after jet multiplicity selections, separately for the two $\ell^+\ell^-$ and for all combined dilepton channels, in figures 1 and 2, respectively. The ratio of the data to the sum of simulations for the signal and backgrounds are shown in the bottom panels of each of the figures. The corresponding $M_{\ell\ell}$ and $\not{E}_{\rm T}$ distributions and their ratios to expectations are shown, respectively, in figures 3 and 4, separately for the combined two $\ell^+\ell^-$ channels and for the $e^\pm\mu^\mp$ channel. The multiplicity of selected jets is presented in figure 5, after applying the dilepton and $\not{E}_{\rm T}$ selections. The observed number of events with less than two jets is used to check the reliability of background predictions. The multiplicity of jets that pass the b-tagging selections is given in figure 6, again separately for the summed e^+e^- and $\mu^+\mu^-$ channels, and for the $e^\pm\mu^\mp$ channel. The observed number of events and the expectation from simulations and data-based predictions are presented in table 3, for a $t\bar{t}$ cross section of 164 pb. The uncertainties shown account for statistical and systematic sources. The predicted and observed number of events are consistent within their uncertainties. Also
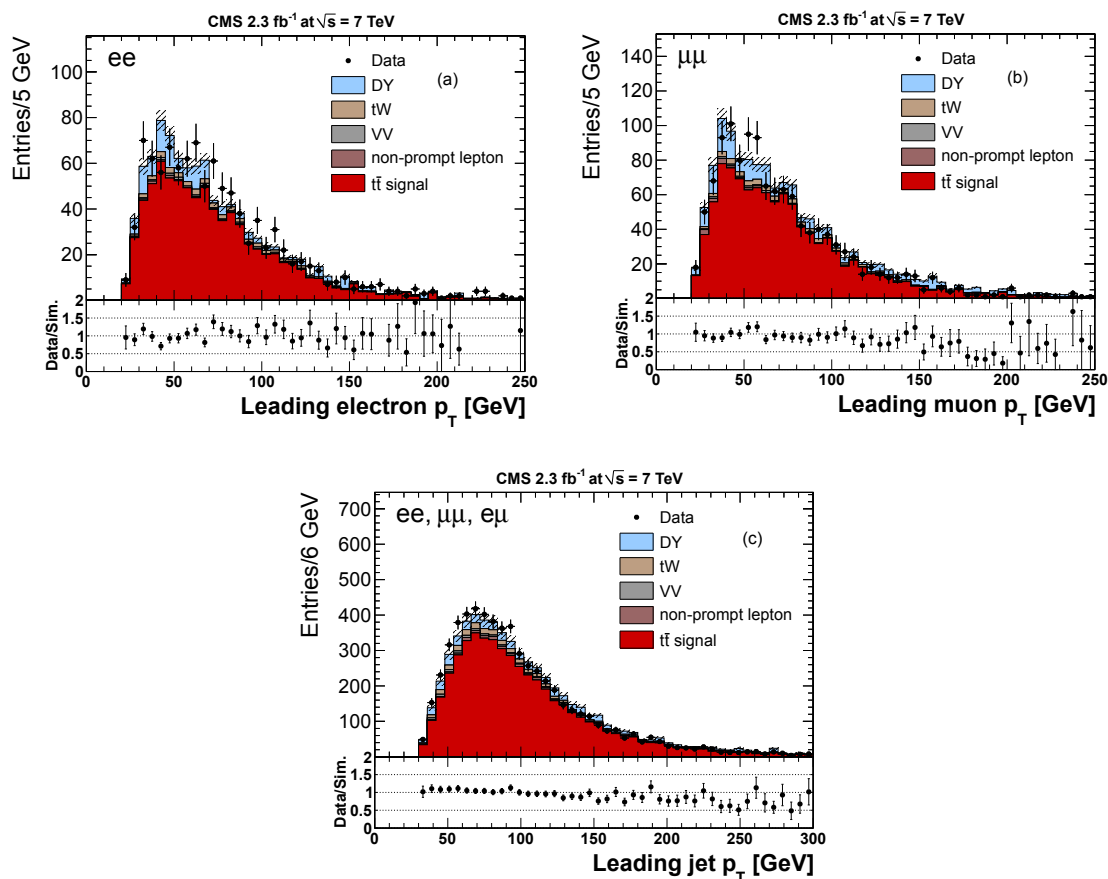
Figure 1. The p_T distributions for (a) electrons, (b) muons, and (c) jets of the largest-p_T after the jet multiplicity selection. The expected distributions for $t\bar{t}$ signal and individual backgrounds are shown by the histograms, and include all data-based corrections. A $t\bar{t}$ cross section of 164 pb is used to normalize the simulated $t\bar{t}$ signal. In this and all following figures, the hatched regions show the total uncertainties on the sum of the $t\bar{t}$ and background predictions. The ratios of data to the sum of the $t\bar{t}$ and background predictions are given at the bottom of each panel and the corresponding error bars include statistic and systematic uncertainties added in quadrature.

shown in table 3 are the acceptances for simulated $t\bar{t}$ signal events, including the two-lepton branching fractions, with and without requiring at least one b-tagged jet.

8   Measuring the $t\bar{t}$ production cross section

The $t\bar{t}$ production cross section is measured using a profile likelihood-ratio method described in section 8.1, while section 8.2 discusses a counting analysis used as a cross-check. The latter is based on counting the number of events in the data that survive an additional selection, which requires at least one b-tagged jet, and is referred to as a counting analysis in what follows. For ease of comparison with previous measurements, the value of $m_t=$
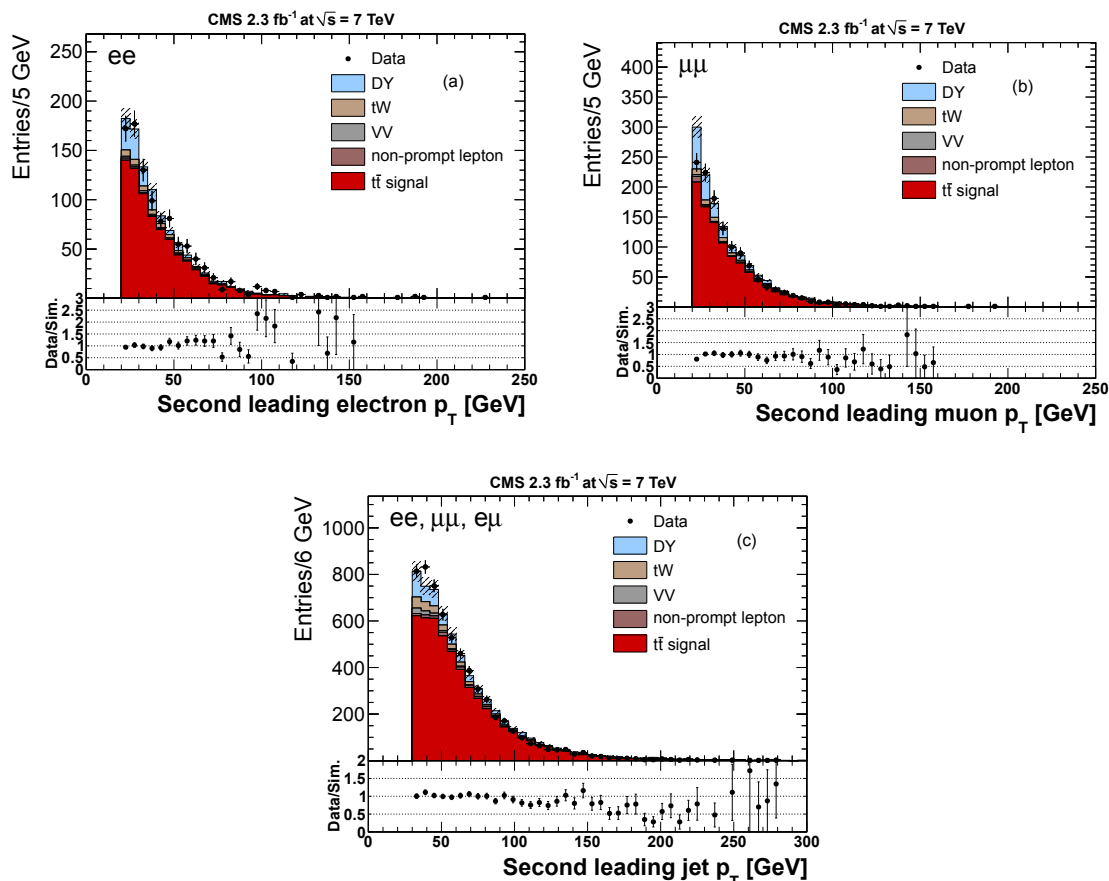
Figure 2. Same as figure 1, but for the second-largest p_T electrons, muons and jets in each event.

172.5 GeV is used to extract the $t\bar{t}$ cross section. The dependence of $\sigma_{t\bar{t}}$ on m_t is discussed in section 8.3.

8.1 Cross-section measurement using a profile likelihood ratio

A profile likelihood ratio [17, 18] is used to measure $\sigma_{t\bar{t}}$ in the individual e^+e^-, $\mu^+\mu^-$, and $e^\pm\mu^\mp$ dilepton channels, as well as in their combination. The minimum value of $-2\ln[\mathcal{R}(\sigma_{t\bar{t}})]$ is extracted from a scan over a wide range of $\sigma_{t\bar{t}}$, where $\mathcal{R}$ is defined as:

$$\mathcal{R}(\sigma_{t\bar{t}}) = \frac{L(\sigma_{t\bar{t}}, \{\hat{\hat{U}}_i\})}{L(\hat{\sigma}_{t\bar{t}}, \{\hat{U}_i\})}, \tag{8.1}$$

with L being the likelihood function with one free parameter, $\sigma_{t\bar{t}}$, and a set of other parameters $\{U_i\}$, called "nuisance parameters", that describe the estimated systematic uncertainties in the measurement. The set $\{\hat{\hat{U}}_i\}$ denotes the conditional maximum-likelihood (ML) estimates of the $\{U_i\}$ that depend on the specific value of $\sigma_{t\bar{t}}$. The denominator corresponds to the maximized unconditional likelihood function, with its ML estimators
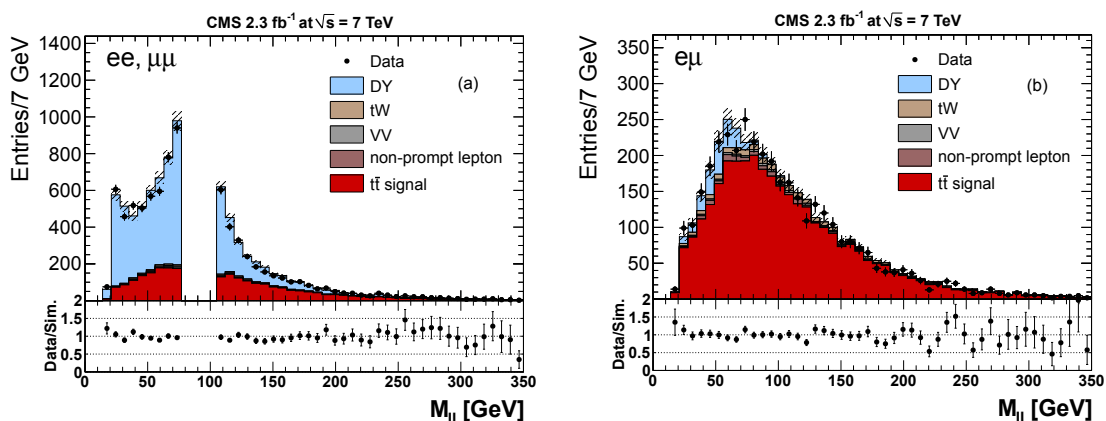
Figure 3. Same as figure 1, but for the dilepton invariant-mass distribution of (a) the sum of the e^+e^- and $\mu^+\mu^-$ channels, and (b) the $e^\pm\mu^\mp$ channel. The gap in the former distribution reflects the requirement that removes dileptons from Z decay.
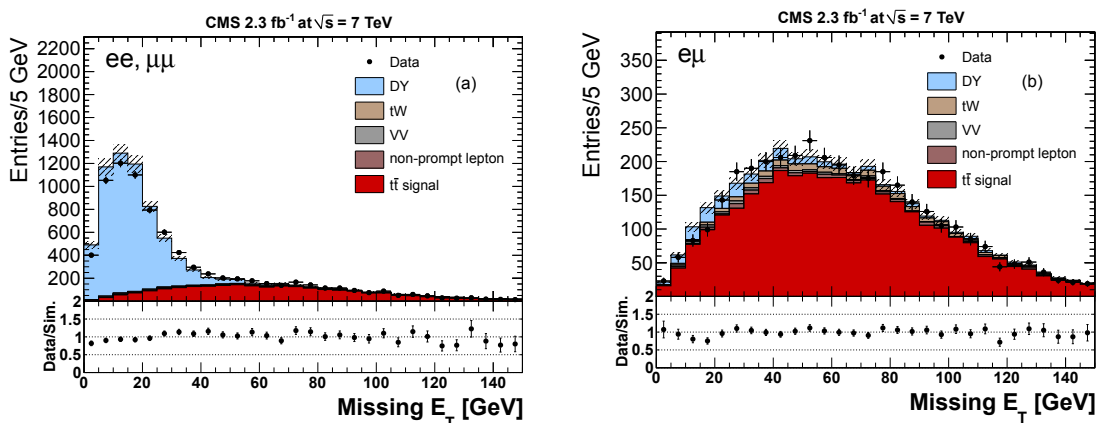

Figure 4. The $\not{E}_T$ distributions after the selection on jet multiplicity. Details on the distributions are same as for figure 1.

defined as $\hat{\sigma}_{t\bar{t}}$ and $\{\hat{U}_i\}$. The presence of the nuisance parameters broadens the distribution of the $\mathcal{R}$ function, which reflects the loss of information on $\sigma_{t\bar{t}}$ from the presence of systematic uncertainties.

We consider a likelihood defined by a probability density function binned in a 2-dimensional (2D) space of jet multiplicity (N_{jets}) and multiplicity of b-tagged jets ($N_{b\text{-jets}}$). The predicted 2D distributions (or "templates") are obtained by applying the event selection criteria to simulated events for each contributing process, without imposing b-tagging requirements. The corresponding number of selected events in simulation, compared with the number selected in data, are shown in figure 7 for different combinations of (N_{jets}, $N_{b\text{-jets}}$).
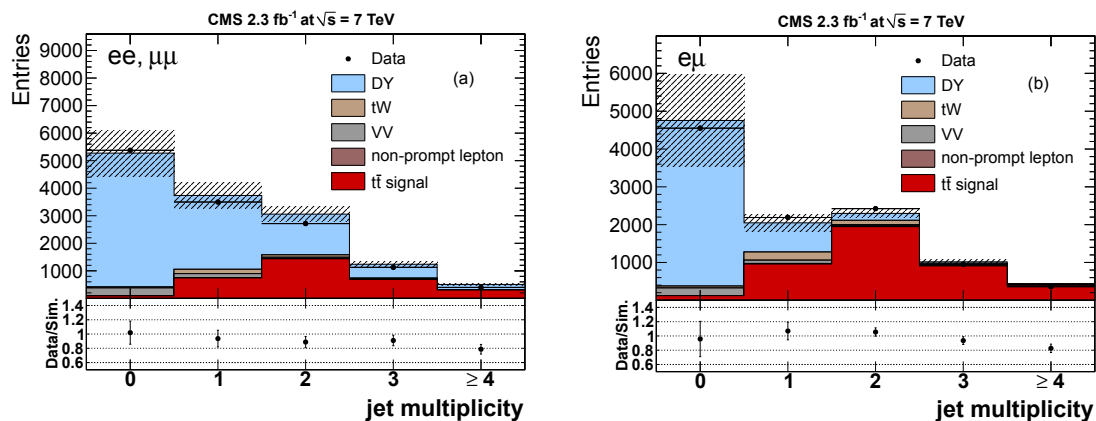
Figure 5. The jet multiplicity for events passing the dilepton and $\not{E}_T$ criteria, but before the b-tagging requirement, for (a) the sum of e^+e^- and $\mu^+\mu^-$ channels, and (b) the $e^\pm\mu^\mp$ channel.
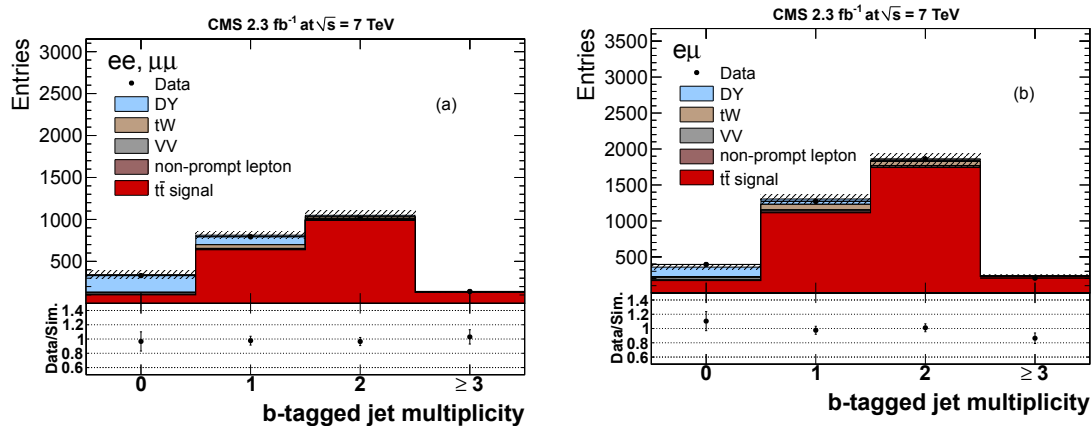

Figure 6. The multiplicity of b-tagged jets in events passing full event selections for (a) the summed e^+e^- and $\mu^+\mu^-$ channels, and (b) the $e^\pm\mu^\mp$ channels.

Without systematic uncertainties, the likelihood function represents the product of Poisson distributions that reflect the statistical content of each bin. To incorporate systematic uncertainties, Gaussian terms are introduced for the nuisance parameters into the likelihood function as constraints on $\{U_i\}$. A systematic uncertainty can affect the 2D distribution by changing its normalization and its differential dependence. The effect is estimated by means of an interpolation between the original 2D template and the ones obtained by changing each nuisance parameter U_i by ± 1 standard deviation. For uncertainties on data-to-simulation SF in tagging of b jets and light-flavor jets, the change in template for a given process is computed analytically for each bin of the distribution, according to the combinatorial probability of tagging $N_{\text{b-jets}}$ jets in an event with N_{jets} jets.

– 14 –

	(a) Number of events		
	Without b-tagging selection		
Source	e^+e^-	$\mu^+\mu^-$	$e^\pm\mu^\mp$
Drell-Yan	136±29	217±45	220±46
Nonprompt leptons	9±6	15±7	85±20
Diboson	14±4	16±4	55±13
Single top	42±9	53±11	156±32
Total background	201±31	301±47	516±61
$t\bar{t}$ signal	801±34	1041±43	3253±126
Total predicted	1002±46	1342±64	3769±140
Data	1021	1259	3734
	(b) ≥ 1b-tagged jet		
Source	$\mu^+\mu^-$	e^+e^-	$e^\pm\mu^\mp$
Drell-Yan	62±16	82±21	89±19
Nonprompt leptons	2.4±4.8	10.0±5.5	50±15
Diboson	5.7±1.4	6.1±1.5	22.3±5.3
Single top	37.5±7.8	47.0±9.8	140±29
Total background	108±18	145±24	301±38
$t\bar{t}$ signal	759±33	991±42	3082±122
Total predicted	867±38	1136±48	3383±128
Data	875	1074	3339
	(c) $t\bar{t}$ acceptance $\times$ eff.$\times$ B (%)		
b-tagging selection	e^+e^-	$\mu^+\mu^-$	$e^\pm\mu^\mp$
No selection	0.22±0.01	0.28±0.01	0.87±0.04
≥ 1b-tagged jet	0.20±0.01	0.27±0.01	0.83±0.04

Table 3. Number of dilepton events in the e^+e^-, $\mu^+\mu^-$, and $e^\pm\mu^\mp$ channels after applying the event-selection criteria: (a) without requiring a b-tagged jet, and (b) requiring at least one b-tagged jet. The results are given for the individual sources of background, $t\bar{t}$ signal for $\sigma_{t\bar{t}} = 164\,\text{pb}$, and the data. The uncertainties reflect statistical and systematic uncertainties added in quadrature. Panel (c) gives the $t\bar{t}$ acceptance multiplied by the selection efficiency and by the branching fractions B (in %) of $t\bar{t}$ to two-lepton states, estimated using $t\bar{t}$ simulated events.

The $\mathcal{R}$ function given in eq. (8.1) is used to extract the uncertainty on $\sigma_{t\bar{t}}$ from a change by ±0.5 of the fitted $-2\ln[\mathcal{R}]$ value relative to its minimum. This represents the Gaussian equivalent of 68% confidence for the combined statistical and systematic uncertainties. The minimization of $\ln[\mathcal{R}]$ corresponds to an integration over the parametrized systematic uncertainties (U_i), which also reduces the overall uncertainty on $\sigma_{t\bar{t}}$.

The technique described for a given decay channel can be extended to the combined channels. The e^+e^-, $\mu^+\mu^-$, and $e^\pm\mu^\mp$ channels are statistically independent because they correspond to independent data samples. The likelihood function for the combined channels is expressed therefore as the product of the individual likelihood functions. Correlations
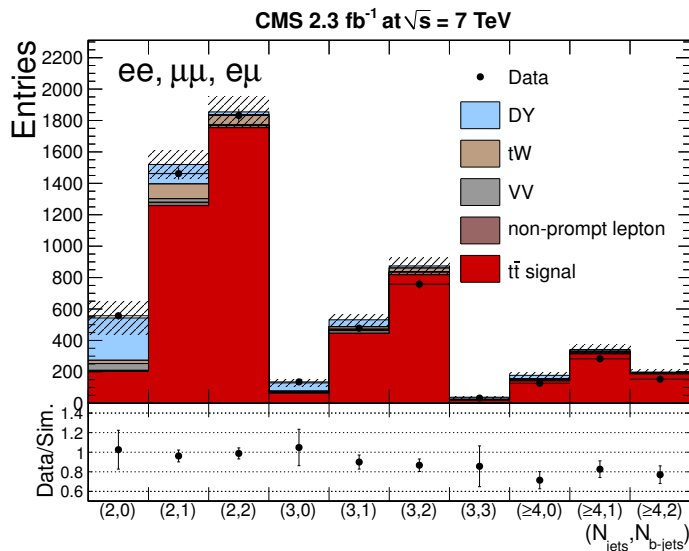
Figure 7. Number of events selected for the three combined dilepton channels, as a function of the number of jets and b-tagged jets (N_{jets}, $N_{\text{b-jets}}$) in each event. The data are shown by the dots, while the predicted $t\bar{t}$ and the contributing backgrounds are shown by the histograms. The hatched area corresponds to statistical and systematic uncertainties on the $t\bar{t}$ and on the background predictions taken in quadrature. The ratios of data to the sum of the $t\bar{t}$ and background predictions are given at the bottom, with the error bars again giving the statistical and systematic uncertainties taken in quadrature.

among the channels are introduced through the nuisance parameters, which are taken to be the same for the e^+e^-, $\mu^+\mu^-$, and $e^\pm\mu^\mp$ channels. The systematic uncertainties included in the PLR analysis are those described in section 6 and summarized in tables 2 and 3.

The results for each dilepton channel and for the combined sample are presented in table 4. The uncertainties reflect statistical and systematic sources, and the uncertainty on integrated luminosity. The measurements from the three dilepton channels are consistent within their uncertainties. The combined result from the PLR method is $161.9 \pm 2.5\,(\text{stat.})\,^{+5.1}_{-5.0}\,(\text{syst.}) \pm 3.6\,(\text{lumi.})\,\text{pb}$.

8.2 Measurement of $\sigma_{t\bar{t}}$ using a counting analysis

The $t\bar{t}$ production cross section is also measured by counting events and applying the expression:

$$\sigma_{t\bar{t}} = \frac{N - N_B}{\mathcal{A}\mathcal{L}}, \tag{8.2}$$

where N is the total number of dilepton events observed in data, N_B is the number of estimated background events, $\mathcal{A}$ is the mean acceptance multiplied by the selection efficiency and by the branching fraction $B(t\bar{t} \to \text{dilepton final state})$, for all produced $t\bar{t}$ events, and $\mathcal{L}$ is the integrated luminosity. The measurement is performed separately for each dilepton channel and the individual channels are combined using a BLUE procedure [50]. While the

Channel	PLR method	Counting analysis
ee	$168.0 \pm 6.6^{+7.6}_{-7.0} \pm 3.7$	$165.9 \pm 6.4 \pm 7.0 \pm 3.6$
$\mu\mu$	$156.3 \pm 5.6^{+7.7}_{-6.6} \pm 3.5$	$153.8 \pm 5.4 \pm 6.6 \pm 3.4$
eμ	$161.9 \pm 3.1^{+5.8}_{-5.4} \pm 3.6$	$161.6 \pm 3.1 \pm 5.6 \pm 3.6$
Combined	$161.9 \pm 2.5^{+5.1}_{-5.0} \pm 3.6$	$161.0 \pm 2.6 \pm 5.6 \pm 3.6$

Table 4. Measured $\sigma_{t\bar{t}}$ in pb for a top quark mass of 172.5 GeV for each of the dilepton channels, as well as for their combination. The quoted uncertainties are, respectively, from statistical and systematic sources and the contributions from integrated luminosity.

PLR method adjusts the jet and the b-tagged jet multiplicities without applying specific b-tagging selections, the counting analysis requires at least one b-tagged jet in an accepted event. This enriches the purity of the $t\bar{t}$ signal in the data sample, but leads to only 5% loss in the number of $t\bar{t}$ events. The values of N, N_B, and $\mathcal{A}$ are given in table 3.

The cross sections measured with this method are given in table 4. As for the PLR method, the systematic uncertainties are described in section 6 and summarized in tables 2 and 3. A breakdown of the statistical and systematic uncertainties contributing to the combined measurement is given in table 5. The measurements agree very well with those based on the PLR method.

Compared to the PLR method, the analysis presented in this section follows an alternative approach that leads to a slightly less sensitive measurement. The PLR and the counting analysis measurements are not combined since they are highly correlated: both are extracted from almost the same data sample, and are affected by essentially the same systematic uncertainties.

8.3 Cross section and mass of the top quark

As the acceptance for $t\bar{t}$ signal depends on the top-quark mass, the measured $t\bar{t}$ cross section also depends on the value of the top-quark mass used to simulate $t\bar{t}$ events. The results presented in table 4 for both the PLR and the counting analysis use a top-quark mass of 172.5 GeV without any additional uncertainties attributed to this quantity.

The dependence of the cross section on m_t in the range 160–185 GeV is studied by measuring $\sigma_{t\bar{t}}$ in $t\bar{t}$ samples simulated at different m_t values. The cross-section dependence can be parametrized as

$$\sigma_{t\bar{t}}/\sigma_{t\bar{t}}(m_t = 172.5) = 1.00 - 0.008 \times (m_t - 172.5) - 0.000137 \times (m_t - 172.5)^2. \quad (8.3)$$

For completeness, the combined cross section is also extracted using the PLR method at the currently accepted value $m_t = 172.9 \pm 0.6\,(\text{stat.}) \pm 0.9\,(\text{syst.})\,\text{GeV}$ [16], which yields a cross section of $\sigma_{t\bar{t}} = 161.3 \pm 2.5\,(\text{stat.})\,^{+5.3}_{-5.2}\,(\text{syst.}) \pm 3.6\,(\text{lumi.})\,\text{pb}$, where the systematic uncertainty also accounts for the uncertainty on the value of m_t.

Source	Uncertainty on $\sigma_{t\bar{t}}$(pb)
Diboson	0.4
Single top	2.3
Drell-Yan	1.0
Non-W/Z leptons	0.6
Lepton efficiencies	1.7
Lepton energy scale	0.5
Jet energy scale	2.8
Jet energy resolution	0.5
$E\!\!\!/_T$ efficiency	1.9
b-tagging	1.1
Pileup	0.7
Scale of QCD (μ)	1.0
Matching partons to showers	1.0
W branching fraction	2.7
Total systematic	5.6
Integrated luminosity	3.6
Statistical	2.6

Table 5. Summary of the individual contributions to the systematic uncertainty on the $\sigma_{t\bar{t}}$ measurement for the combined dilepton sample, using the counting analysis. The uncertainties are given in pb. The statistical uncertainty on the result is given for comparison.

9 Summary

A measurement of the $t\bar{t}$ production cross section at $\sqrt{s} = 7\,\text{TeV}$ is presented for events containing e^+e^-, $\mu^+\mu^-$, or $e^\pm\mu^\mp$ lepton pairs, at least two jets, and a large imbalance in transverse momentum. The measurement is performed using two approaches: a profile likelihood-ratio procedure and an event-counting analysis that relies on the presence of at least one b-tagged jet. The results from the individual dilepton channels and from the two analysis methods are consistent with each other, and are also found to be compatible with previous published measurements. For the profile likelihood-ratio method, the cross section for the combined dilepton channels amounts to $\sigma_{t\bar{t}} = 161.9 \pm 2.5\,\text{(stat.)}\,^{+5.1}_{-5.0}\,\text{(syst.)} \pm 3.6\,\text{(lumi.)}\,\text{pb}$, in agreement with the prediction of the standard model. This result corresponds to the most precise measurement of $\sigma_{t\bar{t}}$ at 7 TeV.

Acknowledgments

References

[1] CMS collaboration, V. Khachatryan et al., *First Measurement of the Cross Section for Top-Quark Pair Production in Proton-Proton Collisions at $\sqrt{s} = 7\,TeV$, Phys. Lett.* **B 695** (2011) 424 [arXiv:1010.5994] [INSPIRE].

[2] ATLAS collaboration, G. Aad et al., *Measurement of the top quark-pair production cross section with ATLAS in pp collisions at $\sqrt{s} = 7$ TeV*, *Eur. Phys. J.* **C 71** (2011) 1577 [arXiv:1012.1792] [INSPIRE].

[3] ATLAS collaboration, G. Aad et al., *Measurement of the cross section for top-quark pair production in pp collisions at $\sqrt{s} = 7$ TeV with the ATLAS detector using final states with two high-p_T leptons*, *JHEP* **05** (2012) 059 [arXiv:1202.4892] [INSPIRE].

[4] ATLAS collaboration, G. Aad et al., *Measurement of the top quark pair production cross-section with ATLAS in the single lepton channel*, *Phys. Lett.* **B 711** (2012) 244 [arXiv:1201.1889] [INSPIRE].

[5] CMS collaboration, S. Chatrchyan et al., *Measurement of the t t-bar production cross section and the top quark mass in the dilepton channel in pp collisions at $\sqrt{s} = 7$ TeV*, *JHEP* **07** (2011) 049 [arXiv:1105.5661] [INSPIRE].

[6] CMS collaboration, S. Chatrchyan et al., *Measurement of the Top-antitop Production Cross Section in pp Collisions at $\sqrt{s} = 7$ TeV using the Kinematic Properties of Events with Leptons and Jets*, *Eur. Phys. J.* **C 71** (2011) 1721 [arXiv:1106.0902] [INSPIRE].

[7] CMS collaboration, S. Chatrchyan et al., *Measurement of the $t\bar{t}$ Production Cross Section in pp Collisions at 7 TeV in Lepton + Jets Events Using b-quark Jet Identification*, *Phys. Rev.* **D 84** (2011) 092004 [arXiv:1108.3773] [INSPIRE].

[8] ATLAS collaboration, G. Aad et al., *Evidence for the associated production of a W boson and a top quark in ATLAS at $\sqrt{s} = 7$ TeV*, *Phys. Lett.* **B 716** (2012) 142 [arXiv:1205.5764] [INSPIRE].

[9] CMS collaboration, S. Chatrchyan et al., *Measurement of the t-channel single top quark production cross section in pp collisions at $\sqrt{s} = 7$ TeV*, *Phys. Rev. Lett.* **107** (2011) 091802 [arXiv:1106.3052] [INSPIRE].

[10] ATLAS collaboration, G. Aad et al., *Measurement of the t-channel single top-quark production cross section in pp collisions at $\sqrt{s} = 7$ TeV with the ATLAS detector*, *Physics Letters B* **717** (2012) 330 [arXiv:1205.3130] [INSPIRE].

[11] CMS collaboration, S. Chatrchyan et al., *Measurement of the charge asymmetry in top-quark pair production in proton-proton collisions at $\sqrt{s} = 7$ TeV*, *Phys. Lett.* **B 709** (2012) 28 [arXiv:1112.5100] [INSPIRE].

[12] ATLAS collaboration, G. Aad et al., *Search for anomalous production of prompt like-sign muon pairs and constraints on physics beyond the Standard Model with the ATLAS detector*, *Phys. Rev.* **D 85** (2012) 032004 [arXiv:1201.1091] [INSPIRE].

[13] ATLAS collaboration, G. Aad et al., *Search for New Phenomena in ttbar Events With Large Missing Transverse Momentum in Proton-Proton Collisions at $\sqrt{s} = 7$ TeV with the ATLAS Detector*, *Phys. Rev. Lett.* **108** (2012) 041805 [arXiv:1109.4725] [INSPIRE].

[14] CMS collaboration, S. Chatrchyan et al., *The CMS experiment at the CERN LHC*, 2008 *JINST* **3** S08004 [INSPIRE].

[15] CMS collaboration, S. Chatrchyan et al., *Measurement of the top quark pair production cross section in pp collisions at $\sqrt{s} = 7$ TeV in dilepton final states containing a τ*, *Phys. Rev.* **D 85** (2012) 112007 [arXiv:1203.6810] [INSPIRE].

[16] PARTICLE DATA GROUP collaboration, J. Beringer et al., *Review of Particle Physics (RPP)*, *Phys. Rev.* **D 86** (2012) 010001 [INSPIRE].

[17] A. Stuart, K. Ord and S. Arnold, *Kendall's advanced theory of statistics. Volume 2A: classical inference and the linear model*, Hodder Arnold (1999).

[18] G. Cowan, K. Cranmer, E. Gross and O. Vitells, *Asymptotic formulae for likelihood-based tests of new physics*, *Eur. Phys. J.* **C 71** (2011) 1554 [arXiv:1007.1727] [INSPIRE].

[19] J.M. Campbell and R. Ellis, *MCFM for the Tevatron and the LHC*, *Nucl. Phys. Proc. Suppl.* **205-206** (2010) 10 [arXiv:1007.3492] [INSPIRE].

[20] R. Kleiss and W.J. Stirling, *Top quark production at hadron colliders: some useful formulae*, *Z. Phys.* **C 40** (1988) 419 [INSPIRE].

[21] N. Kidonakis, *Next-to-next-to-leading soft-gluon corrections for the top quark cross section and transverse momentum distribution*, *Phys. Rev.* **D 82** (2010) 114030 [arXiv:1009.4935] [INSPIRE].

[22] V. Ahrens, A. Ferroglia, M. Neubert, B.D. Pecjak and L.L. Yang, *Renormalization-Group Improved Predictions for Top-Quark Pair Production at Hadron Colliders*, *JHEP* **09** (2010) 097 [arXiv:1003.5827] [INSPIRE].

[23] M. Aliev et al., *HATHOR: HAdronic Top and Heavy quarks crOss section calculatoR*, *Comput. Phys. Commun.* **182** (2011) 1034 [arXiv:1007.1327] [INSPIRE].

[24] J. Alwall, M. Herquet, F. Maltoni, O. Mattelaer and T. Stelzer, *MadGraph 5 : Going Beyond*, *JHEP* **06** (2011) 128 [arXiv:1106.0522] [INSPIRE].

[25] S. Frixione, P. Nason and C. Oleari, *Matching NLO QCD computations with Parton Shower simulations: the POWHEG method*, *JHEP* **11** (2007) 070 [arXiv:0709.2092] [INSPIRE].

[26] T. Sjöstrand, S. Mrenna and P.Z. Skands, *PYTHIA 6.4 Physics and Manual*, *JHEP* **05** (2006) 026 [hep-ph/0603175] [INSPIRE].

[27] N. Davidson, G. Nanava, T. Przedzinski, E. Richter-Was and Z. Was, *Universal Interface of TAUOLA Technical and Physics Documentation*, *Comput. Phys. Commun.* **183** (2012) 821 [arXiv:1002.0543] [INSPIRE].

[28] K. Melnikov and F. Petriello, *Electroweak gauge boson production at hadron colliders through $O(\alpha_s^2)$*, *Phys. Rev.* **D 74** (2006) 114017 [hep-ph/0609070] [INSPIRE].

[29] N. Kidonakis, *Two-loop soft anomalous dimensions for single top quark associated production with a W^- or H^-*, *Phys. Rev.* **D 82** (2010) 054018 [arXiv:1005.4451] [INSPIRE].

[30] CMS collaboration, S. Chatrchyan et al., *Measurement of W^+W^- Production and Search for the Higgs Boson in pp Collisions at $\sqrt{s} = 7\,TeV$*, *Phys. Lett.* **B 699** (2011) 25 [arXiv:1102.5429] [INSPIRE].

[31] ATLAS collaboration, G. Aad et al., *Measurement of the WW cross section in $\sqrt{s} = 7\,TeV$ pp collisions with the ATLAS detector and limits on anomalous gauge couplings*, *Phys. Lett.* **B 712** (2012) 289 [arXiv:1203.6232] [INSPIRE].

[32] ATLAS collaboration, G. Aad et al., *Measurement of the WZ production cross section and limits on anomalous triple gauge couplings in proton-proton collisions at $\sqrt{s} = 7\,TeV$ with the ATLAS detector*, *Phys. Lett.* **B 709** (2012) 341 [arXiv:1111.5570] [INSPIRE].

[33] ATLAS collaboration, G. Aad et al., *Measurement of the ZZ production cross section and limits on anomalous neutral triple gauge couplings in proton-proton collisions at $\sqrt{s} = 7\,TeV$ with the ATLAS detector*, *Phys. Rev. Lett.* **108** (2012) 041804 [arXiv:1110.5016] [INSPIRE].

[34] J. Allison, K. Amako, J. Apostolakis, H. Araujo, P. Dubois, et al., *Geant4 developments and applications*, *IEEE T. Nucl. Sci.* **53** (2006) 270 [INSPIRE].

[35] CMS collaboration, V. Khachatryan et al., *CMS Tracking Performance Results from early LHC Operation*, *Eur. Phys. J.* **C 70** (2010) 1165 [arXiv:1007.1988] [INSPIRE].

[36] CMS collaboration, *Electron reconstruction and identification at $\sqrt{s} = 7\,TeV$*, PAS-EGM-10-004.

[37] CMS collaboration, S. Chatrchyan et al., *Performance of CMS muon reconstruction in pp collision events at $\sqrt{s} = 7\,TeV$*, 2012 *JINST* **7** P10002 [arXiv:1206.4071] [INSPIRE].

[38] CMS collaboration, *Commissioning of the Particle-Flow reconstruction in Minimum-Bias and Jet Events from pp Collisions at 7 TeV*, PAS-PFT-10-002.

[39] CMS collaboration, S. Chatrchyan et al., *Measurement of the Drell-Yan Cross Section in pp Collisions at $\sqrt{s} = 7\,TeV$*, *JHEP* **10** (2011) 007 [arXiv:1108.0566] [INSPIRE].

[40] M. Cacciari, G.P. Salam and G. Soyez, *The Anti-k_t jet clustering algorithm*, *JHEP* **04** (2008) 063 [arXiv:0802.1189] [INSPIRE].

[41] CMS collaboration, *Jet Performance in pp Collisions at 7 TeV*, PAS-JME-10-003.

[42] M. Cacciari, G.P. Salam and G. Soyez, *The Catchment Area of Jets*, *JHEP* **04** (2008) 005 [arXiv:0802.1188] [INSPIRE].

[43] M. Cacciari and G.P. Salam, *Pileup subtraction using jet areas*, *Phys. Lett.* **B 659** (2008) 119 [arXiv:0707.1378] [INSPIRE].

[44] CMS collaboration, *CMS MET Performance in Events Containing Electroweak Bosons from pp Collisions at $\sqrt{s} = 7\,TeV$*, PAS-JME-10-005.

[45] CMS collaboration, *b-Jet Identification in the CMS Experiment*, PAS-BTV-11-004.

[46] CMS collaboration, *Measurement of btagging efficiency using ttbar events*, PAS-BTV-11-003.

[47] CMS collaboration, *Absolute Calibration of Luminosity Measurement at CMS: Summer 2011 Update*, PAS-EWK-11-001.

[48] CMS collaboration, *Jet Energy Corrections determination at 7 TeV*, PAS-JME-10-010.

[49] G. Antchev et al., *First measurement of the total proton-proton cross section at the LHC energy of $\sqrt{s} = 7\,TeV$*, *Europhys. Lett.* **96** (2011) 21002 [arXiv:1110.1395] [INSPIRE].

[50] L. Lyons, D. Gibaut and P. Clifford, *How to combine correlated estimates of a single physical quantity*, *Nucl. Instrum. Meth.* **A 270** (1988) 110 [INSPIRE].

The CMS collaboration

Yerevan Physics Institute, Yerevan, Armenia

S. Chatrchyan, V. Khachatryan, A.M. Sirunyan, A. Tumasyan

Institut für Hochenergiephysik der OeAW, Wien, Austria

W. Adam, E. Aguilo, T. Bergauer, M. Dragicevic, J. Erö, C. Fabjan[1], M. Friedl, R. Frühwirth[1], V.M. Ghete, J. Hammer, N. Hörmann, J. Hrubec, M. Jeitler[1], W. Kiesenhofer, V. Knünz, M. Krammer[1], I. Krätschmer, D. Liko, I. Mikulec, M. Pernicka[†], B. Rahbaran, C. Rohringer, H. Rohringer, R. Schöfbeck, J. Strauss, A. Taurok, W. Waltenberger, G. Walzel, E. Widl, C.-E. Wulz[1]

National Centre for Particle and High Energy Physics, Minsk, Belarus

V. Mossolov, N. Shumeiko, J. Suarez Gonzalez

Universiteit Antwerpen, Antwerpen, Belgium

S. Bansal, T. Cornelis, E.A. De Wolf, X. Janssen, S. Luyckx, L. Mucibello, S. Ochesanu, B. Roland, R. Rougny, M. Selvaggi, Z. Staykova, H. Van Haevermaet, P. Van Mechelen, N. Van Remortel, A. Van Spilbeeck

Vrije Universiteit Brussel, Brussel, Belgium

F. Blekman, S. Blyweert, J. D'Hondt, R. Gonzalez Suarez, A. Kalogeropoulos, M. Maes, A. Olbrechts, W. Van Doninck, P. Van Mulders, G.P. Van Onsem, I. Villella

Université Libre de Bruxelles, Bruxelles, Belgium

B. Clerbaux, G. De Lentdecker, V. Dero, A.P.R. Gay, T. Hreus, A. Léonard, P.E. Marage, T. Reis, L. Thomas, C. Vander Velde, P. Vanlaer, J. Wang

Ghent University, Ghent, Belgium

V. Adler, K. Beernaert, A. Cimmino, S. Costantini, G. Garcia, M. Grunewald, B. Klein, J. Lellouch, A. Marinov, J. Mccartin, A.A. Ocampo Rios, D. Ryckbosch, N. Strobbe, F. Thyssen, M. Tytgat, P. Verwilligen, S. Walsh, E. Yazgan, N. Zaganidis

Université Catholique de Louvain, Louvain-la-Neuve, Belgium

S. Basegmez, G. Bruno, R. Castello, L. Ceard, C. Delaere, T. du Pree, D. Favart, L. Forthomme, A. Giammanco[2], J. Hollar, V. Lemaitre, J. Liao, O. Militaru, C. Nuttens, D. Pagano, A. Pin, K. Piotrzkowski, N. Schul, J.M. Vizan Garcia

Université de Mons, Mons, Belgium

N. Beliy, T. Caebergs, E. Daubie, G.H. Hammad

Centro Brasileiro de Pesquisas Fisicas, Rio de Janeiro, Brazil

G.A. Alves, M. Correa Martins Junior, D. De Jesus Damiao, T. Martins, M.E. Pol, M.H.G. Souza

Universidade do Estado do Rio de Janeiro, Rio de Janeiro, Brazil

W.L. Aldá Júnior, W. Carvalho, A. Custódio, E.M. Da Costa, C. De Oliveira Martins, S. Fonseca De Souza, D. Matos Figueiredo, L. Mundim, H. Nogima, V. Oguri, W.L. Prado Da Silva, A. Santoro, L. Soares Jorge, A. Sznajder

Instituto de Fisica Teorica, Universidade Estadual Paulista, Sao Paulo, Brazil
T.S. Anjos[3], C.A. Bernardes[3], F.A. Dias[4], T.R. Fernandez Perez Tomei, E. M. Gregores[3], C. Lagana, F. Marinho, P.G. Mercadante[3], S.F. Novaes, Sandra S. Padula

Institute for Nuclear Research and Nuclear Energy, Sofia, Bulgaria
V. Genchev[5], P. Iaydjiev[5], S. Piperov, M. Rodozov, S. Stoykova, G. Sultanov, V. Tcholakov, R. Trayanov, M. Vutova

University of Sofia, Sofia, Bulgaria
A. Dimitrov, R. Hadjiiska, V. Kozhuharov, L. Litov, B. Pavlov, P. Petkov

Institute of High Energy Physics, Beijing, China
J.G. Bian, G.M. Chen, H.S. Chen, C.H. Jiang, D. Liang, S. Liang, X. Meng, J. Tao, J. Wang, X. Wang, Z. Wang, H. Xiao, M. Xu, J. Zang, Z. Zhang

State Key Lab. of Nucl. Phys. and Tech., Peking University, Beijing, China
C. Asawatangtrakuldee, Y. Ban, S. Guo, Y. Guo, W. Li, S. Liu, Y. Mao, S.J. Qian, H. Teng, D. Wang, L. Zhang, B. Zhu, W. Zou

Universidad de Los Andes, Bogota, Colombia
C. Avila, J.P. Gomez, B. Gomez Moreno, A.F. Osorio Oliveros, J.C. Sanabria

Technical University of Split, Split, Croatia
N. Godinovic, D. Lelas, R. Plestina[6], D. Polic, I. Puljak[5]

University of Split, Split, Croatia
Z. Antunovic, M. Kovac

Institute Rudjer Boskovic, Zagreb, Croatia
V. Brigljevic, S. Duric, K. Kadija, J. Luetic, S. Morovic

University of Cyprus, Nicosia, Cyprus
A. Attikis, M. Galanti, G. Mavromanolakis, J. Mousa, C. Nicolaou, F. Ptochos, P.A. Razis

Charles University, Prague, Czech Republic
M. Finger, M. Finger Jr.

Academy of Scientific Research and Technology of the Arab Republic of Egypt, Egyptian Network of High Energy Physics, Cairo, Egypt
Y. Assran[7], S. Elgammal[8], A. Ellithi Kamel[9], S. Khalil[8], M.A. Mahmoud[10], A. Radi[11,12]

National Institute of Chemical Physics and Biophysics, Tallinn, Estonia
M. Kadastik, M. Müntel, M. Raidal, L. Rebane, A. Tiko

Department of Physics, University of Helsinki, Helsinki, Finland
P. Eerola, G. Fedi, M. Voutilainen

Helsinki Institute of Physics, Helsinki, Finland
J. Härkönen, A. Heikkinen, V. Karimäki, R. Kinnunen, M.J. Kortelainen, T. Lampén, K. Lassila-Perini, S. Lehti, T. Lindén, P. Luukka, T. Mäenpää, T. Peltola, E. Tuominen, J. Tuominiemi, E. Tuovinen, D. Ungaro, L. Wendland

Lappeenranta University of Technology, Lappeenranta, Finland

K. Banzuzi, A. Karjalainen, A. Korpela, T. Tuuva

DSM/IRFU, CEA/Saclay, Gif-sur-Yvette, France

M. Besancon, S. Choudhury, M. Dejardin, D. Denegri, B. Fabbro, J.L. Faure, F. Ferri, S. Ganjour, A. Givernaud, P. Gras, G. Hamel de Monchenault, P. Jarry, E. Locci, J. Malcles, L. Millischer, A. Nayak, J. Rander, A. Rosowsky, I. Shreyber, M. Titov

Laboratoire Leprince-Ringuet, Ecole Polytechnique, IN2P3-CNRS, Palaiseau, France

S. Baffioni, F. Beaudette, L. Benhabib, L. Bianchini, M. Bluj[13], C. Broutin, P. Busson, C. Charlot, N. Daci, T. Dahms, L. Dobrzynski, R. Granier de Cassagnac, M. Haguenauer, P. Miné, C. Mironov, I.N. Naranjo, M. Nguyen, C. Ochando, P. Paganini, D. Sabes, R. Salerno, Y. Sirois, C. Veelken, A. Zabi

Institut Pluridisciplinaire Hubert Curien, Université de Strasbourg, Université de Haute Alsace Mulhouse, CNRS/IN2P3, Strasbourg, France

J.-L. Agram[14], J. Andrea, D. Bloch, D. Bodin, J.-M. Brom, M. Cardaci, E.C. Chabert, C. Collard, E. Conte[14], F. Drouhin[14], C. Ferro, J.-C. Fontaine[14], D. Gelé, U. Goerlach, P. Juillot, A.-C. Le Bihan, P. Van Hove

Centre de Calcul de l'Institut National de Physique Nucleaire et de Physique des Particules, CNRS/IN2P3, Villeurbanne, France, Villeurbanne, France

F. Fassi, D. Mercier

Université de Lyon, Université Claude Bernard Lyon 1, CNRS-IN2P3, Institut de Physique Nucléaire de Lyon, Villeurbanne, France

S. Beauceron, N. Beaupere, O. Bondu, G. Boudoul, J. Chasserat, R. Chierici[5], D. Contardo, P. Depasse, H. El Mamouni, J. Fay, S. Gascon, M. Gouzevitch, B. Ille, T. Kurca, M. Lethuillier, L. Mirabito, S. Perries, V. Sordini, Y. Tschudi, P. Verdier, S. Viret

Institute of High Energy Physics and Informatization, Tbilisi State University, Tbilisi, Georgia

Z. Tsamalaidze[15]

RWTH Aachen University, I. Physikalisches Institut, Aachen, Germany

G. Anagnostou, S. Beranek, M. Edelhoff, L. Feld, N. Heracleous, O. Hindrichs, R. Jussen, K. Klein, J. Merz, A. Ostapchuk, A. Perieanu, F. Raupach, J. Sammet, S. Schael, D. Sprenger, H. Weber, B. Wittmer, V. Zhukov[16]

RWTH Aachen University, III. Physikalisches Institut A, Aachen, Germany

M. Ata, J. Caudron, E. Dietz-Laursonn, D. Duchardt, M. Erdmann, R. Fischer, A. Güth, T. Hebbeker, C. Heidemann, K. Hoepfner, D. Klingebiel, P. Kreuzer, C. Magass, M. Merschmeyer, A. Meyer, M. Olschewski, P. Papacz, H. Pieta, H. Reithler, S.A. Schmitz, L. Sonnenschein, J. Steggemann, D. Teyssier, M. Weber

RWTH Aachen University, III. Physikalisches Institut B, Aachen, Germany

M. Bontenackels, V. Cherepanov, G. Flügge, H. Geenen, M. Geisler, W. Haj Ahmad, F. Hoehle, B. Kargoll, T. Kress, Y. Kuessel, A. Nowack, L. Perchalla, O. Pooth, P. Sauerland, A. Stahl

Deutsches Elektronen-Synchrotron, Hamburg, Germany

M. Aldaya Martin, J. Behr, W. Behrenhoff, U. Behrens, M. Bergholz[17], A. Bethani, K. Borras, A. Burgmeier, A. Cakir, L. Calligaris, A. Campbell, E. Castro, F. Costanza, D. Dammann, C. Diez Pardos, G. Eckerlin, D. Eckstein, G. Flucke, A. Geiser, I. Glushkov, P. Gunnellini, S. Habib, J. Hauk, G. Hellwig, H. Jung, M. Kasemann, P. Katsas, C. Kleinwort, H. Kluge, A. Knutsson, M. Krämer, D. Krücker, E. Kuznetsova, W. Lange, W. Lohmann[17], B. Lutz, R. Mankel, I. Marfin, M. Marienfeld, I.-A. Melzer-Pellmann, A.B. Meyer, J. Mnich, A. Mussgiller, S. Naumann-Emme, J. Olzem, H. Perrey, A. Petrukhin, D. Pitzl, A. Raspereza, P.M. Ribeiro Cipriano, C. Riedl, E. Ron, M. Rosin, J. Salfeld-Nebgen, R. Schmidt[17], T. Schoerner-Sadenius, N. Sen, A. Spiridonov, M. Stein, R. Walsh, C. Wissing

University of Hamburg, Hamburg, Germany

C. Autermann, V. Blobel, J. Draeger, H. Enderle, J. Erfle, U. Gebbert, M. Görner, T. Hermanns, R.S. Höing, K. Kaschube, G. Kaussen, H. Kirschenmann, R. Klanner, J. Lange, B. Mura, F. Nowak, T. Peiffer, N. Pietsch, D. Rathjens, C. Sander, H. Schettler, P. Schleper, E. Schlieckau, A. Schmidt, M. Schröder, T. Schum, M. Seidel, V. Sola, H. Stadie, G. Steinbrück, J. Thomsen, L. Vanelderen

Institut für Experimentelle Kernphysik, Karlsruhe, Germany

C. Barth, J. Berger, C. Böser, T. Chwalek, W. De Boer, A. Descroix, A. Dierlamm, M. Feindt, M. Guthoff[5], C. Hackstein, F. Hartmann, T. Hauth[5], M. Heinrich, H. Held, K.H. Hoffmann, S. Honc, I. Katkov[16], J.R. Komaragiri, P. Lobelle Pardo, D. Martschei, S. Mueller, Th. Müller, M. Niegel, A. Nürnberg, O. Oberst, A. Oehler, J. Ott, G. Quast, K. Rabbertz, F. Ratnikov, N. Ratnikova, S. Röcker, A. Scheurer, F.-P. Schilling, G. Schott, H.J. Simonis, F.M. Stober, D. Troendle, R. Ulrich, J. Wagner-Kuhr, S. Wayand, T. Weiler, M. Zeise

Institute of Nuclear Physics "Demokritos", Aghia Paraskevi, Greece

G. Daskalakis, T. Geralis, S. Kesisoglou, A. Kyriakis, D. Loukas, I. Manolakos, A. Markou, C. Markou, C. Mavrommatis, E. Ntomari

University of Athens, Athens, Greece

L. Gouskos, T.J. Mertzimekis, A. Panagiotou, N. Saoulidou

University of Ioánnina, Ioánnina, Greece

I. Evangelou, C. Foudas[5], P. Kokkas, N. Manthos, I. Papadopoulos, V. Patras

KFKI Research Institute for Particle and Nuclear Physics, Budapest, Hungary

G. Bencze, C. Hajdu[5], P. Hidas, D. Horvath[18], F. Sikler, V. Veszpremi, G. Vesztergombi[19]

Institute of Nuclear Research ATOMKI, Debrecen, Hungary

N. Beni, S. Czellar, J. Molnar, J. Palinkas, Z. Szillasi

University of Debrecen, Debrecen, Hungary

J. Karancsi, P. Raics, Z.L. Trocsanyi, B. Ujvari

Panjab University, Chandigarh, India

S.B. Beri, V. Bhatnagar, N. Dhingra, R. Gupta, M. Jindal, M. Kaur, M.Z. Mehta, N. Nishu, L.K. Saini, A. Sharma, J. Singh

University of Delhi, Delhi, India

Ashok Kumar, Arun Kumar, S. Ahuja, A. Bhardwaj, B.C. Choudhary, S. Malhotra, M. Naimuddin, K. Ranjan, V. Sharma, R.K. Shivpuri

Saha Institute of Nuclear Physics, Kolkata, India

S. Banerjee, S. Bhattacharya, S. Dutta, B. Gomber, Sa. Jain, Sh. Jain, R. Khurana, S. Sarkar, M. Sharan

Bhabha Atomic Research Centre, Mumbai, India

A. Abdulsalam, R.K. Choudhury, D. Dutta, S. Kailas, V. Kumar, P. Mehta, A.K. Mohanty[5], L.M. Pant, P. Shukla

Tata Institute of Fundamental Research - EHEP, Mumbai, India

T. Aziz, S. Ganguly, M. Guchait[20], M. Maity[21], G. Majumder, K. Mazumdar, G.B. Mohanty, B. Parida, K. Sudhakar, N. Wickramage

Tata Institute of Fundamental Research - HECR, Mumbai, India

S. Banerjee, S. Dugad

Institute for Research in Fundamental Sciences (IPM), Tehran, Iran

H. Arfaei, H. Bakhshiansohi[22], S.M. Etesami[23], A. Fahim[22], M. Hashemi, H. Hesari, A. Jafari[22], M. Khakzad, M. Mohammadi Najafabadi, S. Paktinat Mehdiabadi, B. Safarzadeh[24], M. Zeinali[23]

INFN Sezione di Bari [a]**, Università di Bari** [b]**, Politecnico di Bari** [c]**, Bari, Italy**

M. Abbrescia[a,b], L. Barbone[a,b], C. Calabria[a,b,5], S.S. Chhibra[a,b], A. Colaleo[a], D. Creanza[a,c], N. De Filippis[a,c,5], M. De Palma[a,b], L. Fiore[a], G. Iaselli[a,c], L. Lusito[a,b], G. Maggi[a,c], M. Maggi[a], B. Marangelli[a,b], S. My[a,c], S. Nuzzo[a,b], N. Pacifico[a,b], A. Pompili[a,b], G. Pugliese[a,c], G. Selvaggi[a,b], L. Silvestris[a], G. Singh[a,b], R. Venditti, G. Zito[a]

INFN Sezione di Bologna [a]**, Università di Bologna** [b]**, Bologna, Italy**

G. Abbiendi[a], A.C. Benvenuti[a], D. Bonacorsi[a,b], S. Braibant-Giacomelli[a,b], L. Brigliadori[a,b], P. Capiluppi[a,b], A. Castro[a,b], F.R. Cavallo[a], M. Cuffiani[a,b], G.M. Dallavalle[a], F. Fabbri[a], A. Fanfani[a,b], D. Fasanella[a,b,5], P. Giacomelli[a], C. Grandi[a], L. Guiducci[a,b], S. Marcellini[a], G. Masetti[a], M. Meneghelli[a,b,5], A. Montanari[a], F.L. Navarria[a,b], F. Odorici[a], A. Perrotta[a], F. Primavera[a,b], A.M. Rossi[a,b], T. Rovelli[a,b], G. Siroli[a,b], R. Travaglini[a,b]

INFN Sezione di Catania [a]**, Università di Catania** [b]**, Catania, Italy**

S. Albergo[a,b], G. Cappello[a,b], M. Chiorboli[a,b], S. Costa[a,b], R. Potenza[a,b], A. Tricomi[a,b], C. Tuve[a,b]

INFN Sezione di Firenze [a], **Università di Firenze** [b], **Firenze, Italy**

G. Barbagli[a], V. Ciulli[a,b], C. Civinini[a], R. D'Alessandro[a,b], E. Focardi[a,b], S. Frosali[a,b], E. Gallo[a], S. Gonzi[a,b], M. Meschini[a], S. Paoletti[a], G. Sguazzoni[a], A. Tropiano[a,5]

INFN Laboratori Nazionali di Frascati, Frascati, Italy

L. Benussi, S. Bianco, S. Colafranceschi[25], F. Fabbri, D. Piccolo

INFN Sezione di Genova [a], **Università di Genova** [b], **Genova, Italy**

P. Fabbricatore[a], R. Musenich[a], S. Tosi

INFN Sezione di Milano-Bicocca [a], **Università di Milano-Bicocca** [b], **Milano, Italy**

A. Benaglia[a,b,5], F. De Guio[a,b], L. Di Matteo[a,b,5], S. Fiorendi[a,b], S. Gennai[a,5], A. Ghezzi[a,b], S. Malvezzi[a], R.A. Manzoni[a,b], A. Martelli[a,b], A. Massironi[a,b,5], D. Menasce[a], L. Moroni[a], M. Paganoni[a,b], D. Pedrini[a], S. Ragazzi[a,b], N. Redaelli[a], S. Sala[a], T. Tabarelli de Fatis[a,b]

INFN Sezione di Napoli [a], **Università di Napoli "Federico II"** [b], **Napoli, Italy**

S. Buontempo[a], C.A. Carrillo Montoya[a], N. Cavallo[a,26], A. De Cosa[a,b,5], O. Dogangun[a,b], F. Fabozzi[a,26], A.O.M. Iorio[a], L. Lista[a], S. Meola[a,27], M. Merola[a,b], P. Paolucci[a,5]

INFN Sezione di Padova [a], **Università di Padova** [b], **Università di Trento (Trento)** [c], **Padova, Italy**

P. Azzi[a], N. Bacchetta[a,5], D. Bisello[a,b], A. Branca[a,5], R. Carlin[a,b], P. Checchia[a], T. Dorigo[a], F. Gasparini[a,b], U. Gasparini[a,b], A. Gozzelino[a], K. Kanishchev[a,c], S. Lacaprara[a], I. Lazzizzera[a,c], M. Margoni[a,b], A.T. Meneguzzo[a,b], J. Pazzini[a,b], N. Pozzobon[a,b], P. Ronchese[a,b], F. Simonetto[a,b], E. Torassa[a], M. Tosi[a,b,5], A. Triossi[a], S. Vanini[a,b], P. Zotto[a,b], G. Zumerle[a,b]

INFN Sezione di Pavia [a], **Università di Pavia** [b], **Pavia, Italy**

M. Gabusi[a,b], S.P. Ratti[a,b], C. Riccardi[a,b], P. Torre[a,b], P. Vitulo[a,b]

INFN Sezione di Perugia [a], **Università di Perugia** [b], **Perugia, Italy**

M. Biasini[a,b], G.M. Bilei[a], L. Fanò[a,b], P. Lariccia[a,b], A. Lucaroni[a,b,5], G. Mantovani[a,b], M. Menichelli[a], A. Nappi[a,b], F. Romeo[a,b], A. Saha[a], A. Santocchia[a,b], A. Spiezia[a,b], S. Taroni[a,b,5]

INFN Sezione di Pisa [a], **Università di Pisa** [b], **Scuola Normale Superiore di Pisa** [c], **Pisa, Italy**

P. Azzurri[a,c], G. Bagliesi[a], T. Boccali[a], G. Broccolo[a,c], R. Castaldi[a], R.T. D'Agnolo[a,c], R. Dell'Orso[a], F. Fiori[a,b,5], L. Foà[a,c], A. Giassi[a], A. Kraan[a], F. Ligabue[a,c], T. Lomtadze[a], L. Martini[a,28], A. Messineo[a,b], F. Palla[a], A. Rizzi[a,b], A.T. Serban[a,29], P. Spagnolo[a], P. Squillacioti[a,5], R. Tenchini[a], G. Tonelli[a,b,5], A. Venturi[a,5], P.G. Verdini[a]

INFN Sezione di Roma [a], **Università di Roma "La Sapienza"** [b], **Roma, Italy**

L. Barone[a,b], F. Cavallari[a], D. Del Re[a,b,5], M. Diemoz[a], C. Fanelli, M. Grassi[a,b,5], E. Longo[a,b], P. Meridiani[a,5], F. Micheli[a,b], S. Nourbakhsh[a,b], G. Organtini[a,b], R. Paramatti[a], S. Rahatlou[a,b], M. Sigamani[a], L. Soffi[a,b]

INFN Sezione di Torino ^{a}, Università di Torino ^{b}, Università del Piemonte Orientale (Novara) ^{c}, Torino, Italy

N. Amapane^{a,b}, R. Arcidiacono^{a,c}, S. Argiro^{a,b}, M. Arneodo^{a,c}, C. Biino^a, N. Cartiglia^a, M. Costa^{a,b}, D. Dattola^a, N. Demaria^a, C. Mariotti^{a,5}, S. Maselli^a, E. Migliore^{a,b}, V. Monaco^{a,b}, M. Musich^{a,5}, M.M. Obertino^{a,c}, N. Pastrone^a, M. Pelliccioni^a, A. Potenza^{a,b}, A. Romero^{a,b}, R. Sacchi^{a,b}, A. Solano^{a,b}, A. Staiano^a, A. Vilela Pereira^a

INFN Sezione di Trieste ^{a}, Università di Trieste ^{b}, Trieste, Italy

S. Belforte^a, V. Candelise^{a,b}, F. Cossutti^a, G. Della Ricca^{a,b}, B. Gobbo^a, M. Marone^{a,b,5}, D. Montanino^{a,b,5}, A. Penzo^a, A. Schizzi^{a,b}

Kangwon National University, Chunchon, Korea

S.G. Heo, T.Y. Kim, S.K. Nam

Kyungpook National University, Daegu, Korea

S. Chang, D.H. Kim, G.N. Kim, D.J. Kong, H. Park, S.R. Ro, D.C. Son, T. Son

Chonnam National University, Institute for Universe and Elementary Particles, Kwangju, Korea

J.Y. Kim, Zero J. Kim, S. Song

Korea University, Seoul, Korea

S. Choi, D. Gyun, B. Hong, M. Jo, H. Kim, T.J. Kim, K.S. Lee, D.H. Moon, S.K. Park

University of Seoul, Seoul, Korea

M. Choi, J.H. Kim, C. Park, I.C. Park, S. Park, G. Ryu

Sungkyunkwan University, Suwon, Korea

Y. Cho, Y. Choi, Y.K. Choi, J. Goh, M.S. Kim, E. Kwon, B. Lee, J. Lee, S. Lee, H. Seo, I. Yu

Vilnius University, Vilnius, Lithuania

M.J. Bilinskas, I. Grigelionis, M. Janulis, A. Juodagalvis

Centro de Investigacion y de Estudios Avanzados del IPN, Mexico City, Mexico

H. Castilla-Valdez, E. De La Cruz-Burelo, I. Heredia-de La Cruz, R. Lopez-Fernandez, R. Magaña Villalba, J. Martínez-Ortega, A. Sánchez-Hernández, L.M. Villasenor-Cendejas

Universidad Iberoamericana, Mexico City, Mexico

S. Carrillo Moreno, F. Vazquez Valencia

Benemerita Universidad Autonoma de Puebla, Puebla, Mexico

H.A. Salazar Ibarguen

Universidad Autónoma de San Luis Potosí, San Luis Potosí, Mexico

E. Casimiro Linares, A. Morelos Pineda, M.A. Reyes-Santos

University of Auckland, Auckland, New Zealand

D. Krofcheck

University of Canterbury, Christchurch, New Zealand

A.J. Bell, P.H. Butler, R. Doesburg, S. Reucroft, H. Silverwood

National Centre for Physics, Quaid-I-Azam University, Islamabad, Pakistan

M. Ahmad, M.I. Asghar, H.R. Hoorani, S. Khalid, W.A. Khan, T. Khurshid, S. Qazi, M.A. Shah, M. Shoaib

National Centre for Nuclear Research, Swierk, Poland

H. Bialkowska, B. Boimska, T. Frueboes, R. Gokieli, M. Górski, M. Kazana, K. Nawrocki, K. Romanowska-Rybinska, M. Szleper, G. Wrochna, P. Zalewski

Institute of Experimental Physics, Faculty of Physics, University of Warsaw, Warsaw, Poland

G. Brona, K. Bunkowski, M. Cwiok, W. Dominik, K. Doroba, A. Kalinowski, M. Konecki, J. Krolikowski

Laboratório de Instrumentação e Física Experimental de Partículas, Lisboa, Portugal

N. Almeida, P. Bargassa, A. David, P. Faccioli, P.G. Ferreira Parracho, M. Gallinaro, J. Seixas, J. Varela, P. Vischia

Joint Institute for Nuclear Research, Dubna, Russia

I. Belotelov, P. Bunin, M. Gavrilenko, I. Golutvin, I. Gorbunov, A. Kamenev, V. Karjavin, G. Kozlov, A. Lanev, A. Malakhov, P. Moisenz, V. Palichik, V. Perelygin, S. Shmatov, V. Smirnov, A. Volodko, A. Zarubin

Petersburg Nuclear Physics Institute, Gatchina (St Petersburg), Russia

S. Evstyukhin, V. Golovtsov, Y. Ivanov, V. Kim, P. Levchenko, V. Murzin, V. Oreshkin, I. Smirnov, V. Sulimov, L. Uvarov, S. Vavilov, A. Vorobyev, An. Vorobyev

Institute for Nuclear Research, Moscow, Russia

Yu. Andreev, A. Dermenev, S. Gninenko, N. Golubev, M. Kirsanov, N. Krasnikov, V. Matveev, A. Pashenkov, D. Tlisov, A. Toropin

Institute for Theoretical and Experimental Physics, Moscow, Russia

V. Epshteyn, M. Erofeeva, V. Gavrilov, M. Kossov[5], N. Lychkovskaya, V. Popov, G. Safronov, S. Semenov, V. Stolin, E. Vlasov, A. Zhokin

Moscow State University, Moscow, Russia

A. Belyaev, E. Boos, V. Bunichev, M. Dubinin[4], L. Dudko, A. Ershov, A. Gribushin, V. Klyukhin, O. Kodolova, I. Lokhtin, A. Markina, S. Obraztsov, M. Perfilov, A. Popov, L. Sarycheva[†], V. Savrin, A. Snigirev

P.N. Lebedev Physical Institute, Moscow, Russia

V. Andreev, M. Azarkin, I. Dremin, M. Kirakosyan, A. Leonidov, G. Mesyats, S.V. Rusakov, A. Vinogradov

State Research Center of Russian Federation, Institute for High Energy Physics, Protvino, Russia

I. Azhgirey, I. Bayshev, S. Bitioukov, V. Grishin[5], V. Kachanov, D. Konstantinov, A. Korablev, V. Krychkine, V. Petrov, R. Ryutin, A. Sobol, L. Tourtchanovitch, S. Troshin, N. Tyurin, A. Uzunian, A. Volkov

University of Belgrade, Faculty of Physics and Vinca Institute of Nuclear Sciences, Belgrade, Serbia

P. Adzic[30], M. Djordjevic, M. Ekmedzic, D. Krpic[30], J. Milosevic

Centro de Investigaciones Energéticas Medioambientales y Tecnológicas (CIEMAT), Madrid, Spain

M. Aguilar-Benitez, J. Alcaraz Maestre, P. Arce, C. Battilana, E. Calvo, M. Cerrada, M. Chamizo Llatas, N. Colino, B. De La Cruz, A. Delgado Peris, D. Domínguez Vázquez, C. Fernandez Bedoya, J.P. Fernández Ramos, A. Ferrando, J. Flix, M.C. Fouz, P. Garcia-Abia, O. Gonzalez Lopez, S. Goy Lopez, J.M. Hernandez, M.I. Josa, G. Merino, J. Puerta Pelayo, A. Quintario Olmeda, I. Redondo, L. Romero, J. Santaolalla, M.S. Soares, C. Willmott

Universidad Autónoma de Madrid, Madrid, Spain

C. Albajar, G. Codispoti, J.F. de Trocóniz

Universidad de Oviedo, Oviedo, Spain

H. Brun, J. Cuevas, J. Fernandez Menendez, S. Folgueras, I. Gonzalez Caballero, L. Lloret Iglesias, J. Piedra Gomez

Instituto de Física de Cantabria (IFCA), CSIC-Universidad de Cantabria, Santander, Spain

J.A. Brochero Cifuentes, I.J. Cabrillo, A. Calderon, S.H. Chuang, J. Duarte Campderros, M. Felcini[31], M. Fernandez, G. Gomez, J. Gonzalez Sanchez, A. Graziano, C. Jorda, A. Lopez Virto, J. Marco, R. Marco, C. Martinez Rivero, F. Matorras, F.J. Munoz Sanchez, T. Rodrigo, A.Y. Rodríguez-Marrero, A. Ruiz-Jimeno, L. Scodellaro, M. Sobron Sanudo, I. Vila, R. Vilar Cortabitarte

CERN, European Organization for Nuclear Research, Geneva, Switzerland

D. Abbaneo, E. Auffray, G. Auzinger, P. Baillon, A.H. Ball, D. Barney, J.F. Benitez, C. Bernet[6], G. Bianchi, P. Bloch, A. Bocci, A. Bonato, C. Botta, H. Breuker, T. Camporesi, G. Cerminara, T. Christiansen, J.A. Coarasa Perez, D. D'Enterria, A. Dabrowski, A. De Roeck, S. Di Guida, M. Dobson, N. Dupont-Sagorin, A. Elliott-Peisert, B. Frisch, W. Funk, G. Georgiou, M. Giffels, D. Gigi, K. Gill, D. Giordano, M. Giunta, F. Glege, R. Gomez-Reino Garrido, P. Govoni, S. Gowdy, R. Guida, M. Hansen, P. Harris, C. Hartl, J. Harvey, B. Hegner, A. Hinzmann, V. Innocente, P. Janot, K. Kaadze, E. Karavakis, K. Kousouris, P. Lecoq, Y.-J. Lee, P. Lenzi, C. Lourenço, T. Mäki, M. Malberti, L. Malgeri, M. Mannelli, L. Masetti, F. Meijers, S. Mersi, E. Meschi, R. Moser, M.U. Mozer, M. Mulders, P. Musella, E. Nesvold, T. Orimoto, L. Orsini, E. Palencia Cortezon, E. Perez, L. Perrozzi, A. Petrilli, A. Pfeiffer, M. Pierini, M. Pimiä, D. Piparo, G. Polese, L. Quertenmont,

A. Racz, W. Reece, J. Rodrigues Antunes, G. Rolandi[32], T. Rommerskirchen, C. Rovelli[33], M. Rovere, H. Sakulin, F. Santanastasio, C. Schäfer, C. Schwick, I. Segoni, S. Sekmen, A. Sharma, P. Siegrist, P. Silva, M. Simon, P. Sphicas[34], D. Spiga, A. Tsirou, G.I. Veres[19], J.R. Vlimant, H.K. Wöhri, S.D. Worm[35], W.D. Zeuner

Paul Scherrer Institut, Villigen, Switzerland

W. Bertl, K. Deiters, W. Erdmann, K. Gabathuler, R. Horisberger, Q. Ingram, H.C. Kaestli, S. König, D. Kotlinski, U. Langenegger, F. Meier, D. Renker, T. Rohe, J. Sibille[36]

Institute for Particle Physics, ETH Zurich, Zurich, Switzerland

L. Bäni, P. Bortignon, M.A. Buchmann, B. Casal, N. Chanon, A. Deisher, G. Dissertori, M. Dittmar, M. Donegà, M. Dünser, J. Eugster, K. Freudenreich, C. Grab, D. Hits, P. Lecomte, W. Lustermann, A.C. Marini, P. Martinez Ruiz del Arbol, N. Mohr, F. Moortgat, C. Nägeli[37], P. Nef, F. Nessi-Tedaldi, F. Pandolfi, L. Pape, F. Pauss, M. Peruzzi, F.J. Ronga, M. Rossini, L. Sala, A.K. Sanchez, A. Starodumov[38], B. Stieger, M. Takahashi, L. Tauscher[†], A. Thea, K. Theofilatos, D. Treille, C. Urscheler, R. Wallny, H.A. Weber, L. Wehrli

Universität Zürich, Zurich, Switzerland

C. Amsler, V. Chiochia, S. De Visscher, C. Favaro, M. Ivova Rikova, B. Millan Mejias, P. Otiougova, P. Robmann, H. Snoek, S. Tupputi, M. Verzetti

National Central University, Chung-Li, Taiwan

Y.H. Chang, K.H. Chen, C.M. Kuo, S.W. Li, W. Lin, Z.K. Liu, Y.J. Lu, D. Mekterovic, A.P. Singh, R. Volpe, S.S. Yu

National Taiwan University (NTU), Taipei, Taiwan

P. Bartalini, P. Chang, Y.H. Chang, Y.W. Chang, Y. Chao, K.F. Chen, C. Dietz, U. Grundler, W.-S. Hou, Y. Hsiung, K.Y. Kao, Y.J. Lei, R.-S. Lu, D. Majumder, E. Petrakou, X. Shi, J.G. Shiu, Y.M. Tzeng, X. Wan, M. Wang

Cukurova University, Adana, Turkey

A. Adiguzel, M.N. Bakirci[39], S. Cerci[40], C. Dozen, I. Dumanoglu, E. Eskut, S. Girgis, G. Gokbulut, E. Gurpinar, I. Hos, E.E. Kangal, T. Karaman, G. Karapinar[41], A. Kayis Topaksu, G. Onengut, K. Ozdemir, S. Ozturk[42], A. Polatoz, K. Sogut[43], D. Sunar Cerci[40], B. Tali[40], H. Topakli[39], L.N. Vergili, M. Vergili

Middle East Technical University, Physics Department, Ankara, Turkey

I.V. Akin, T. Aliev, B. Bilin, S. Bilmis, M. Deniz, H. Gamsizkan, A.M. Guler, K. Ocalan, A. Ozpineci, M. Serin, R. Sever, U.E. Surat, M. Yalvac, E. Yildirim, M. Zeyrek

Bogazici University, Istanbul, Turkey

E. Gülmez, B. Isildak[44], M. Kaya[45], O. Kaya[45], S. Ozkorucuklu[46], N. Sonmez[47]

Istanbul Technical University, Istanbul, Turkey

K. Cankocak

National Scientific Center, Kharkov Institute of Physics and Technology, Kharkov, Ukraine

L. Levchuk

University of Bristol, Bristol, United Kingdom

F. Bostock, J.J. Brooke, E. Clement, D. Cussans, H. Flacher, R. Frazier, J. Goldstein, M. Grimes, G.P. Heath, H.F. Heath, L. Kreczko, S. Metson, D.M. Newbold[35], K. Nirunpong, A. Poll, S. Senkin, V.J. Smith, T. Williams

Rutherford Appleton Laboratory, Didcot, United Kingdom

L. Basso[48], K.W. Bell, A. Belyaev[48], C. Brew, R.M. Brown, D.J.A. Cockerill, J.A. Coughlan, K. Harder, S. Harper, J. Jackson, B.W. Kennedy, E. Olaiya, D. Petyt, B.C. Radburn-Smith, C.H. Shepherd-Themistocleous, I.R. Tomalin, W.J. Womersley

Imperial College, London, United Kingdom

R. Bainbridge, G. Ball, R. Beuselinck, O. Buchmuller, D. Colling, N. Cripps, M. Cutajar, P. Dauncey, G. Davies, M. Della Negra, W. Ferguson, J. Fulcher, D. Futyan, A. Gilbert, A. Guneratne Bryer, G. Hall, Z. Hatherell, J. Hays, G. Iles, M. Jarvis, G. Karapostoli, L. Lyons, A.-M. Magnan, J. Marrouche, B. Mathias, R. Nandi, J. Nash, A. Nikitenko[38], A. Papageorgiou, J. Pela[5], M. Pesaresi, K. Petridis, M. Pioppi[49], D.M. Raymond, S. Rogerson, A. Rose, M.J. Ryan, C. Seez, P. Sharp[†], A. Sparrow, M. Stoye, A. Tapper, M. Vazquez Acosta, T. Virdee, S. Wakefield, N. Wardle, T. Whyntie

Brunel University, Uxbridge, United Kingdom

M. Chadwick, J.E. Cole, P.R. Hobson, A. Khan, P. Kyberd, D. Leggat, D. Leslie, W. Martin, I.D. Reid, P. Symonds, L. Teodorescu, M. Turner

Baylor University, Waco, USA

K. Hatakeyama, H. Liu, T. Scarborough

The University of Alabama, Tuscaloosa, USA

O. Charaf, C. Henderson, P. Rumerio

Boston University, Boston, USA

A. Avetisyan, T. Bose, C. Fantasia, A. Heister, J. St. John, P. Lawson, D. Lazic, J. Rohlf, D. Sperka, L. Sulak

Brown University, Providence, USA

J. Alimena, S. Bhattacharya, D. Cutts, A. Ferapontov, U. Heintz, S. Jabeen, G. Kukartsev, E. Laird, G. Landsberg, M. Luk, M. Narain, D. Nguyen, M. Segala, T. Sinthuprasith, T. Speer, K.V. Tsang

University of California, Davis, Davis, USA

R. Breedon, G. Breto, M. Calderon De La Barca Sanchez, S. Chauhan, M. Chertok, J. Conway, R. Conway, P.T. Cox, J. Dolen, R. Erbacher, M. Gardner, R. Houtz, W. Ko, A. Kopecky, R. Lander, T. Miceli, D. Pellett, F. Ricci-tam, B. Rutherford, M. Searle, J. Smith, M. Squires, M. Tripathi, R. Vasquez Sierra

University of California, Los Angeles, Los Angeles, USA

V. Andreev, D. Cline, R. Cousins, J. Duris, S. Erhan, P. Everaerts, C. Farrell, J. Hauser, M. Ignatenko, C. Jarvis, C. Plager, G. Rakness, P. Schlein[†], P. Traczyk, V. Valuev, M. Weber

University of California, Riverside, Riverside, USA

J. Babb, R. Clare, M.E. Dinardo, J. Ellison, J.W. Gary, F. Giordano, G. Hanson, G.Y. Jeng[50], H. Liu, O.R. Long, A. Luthra, H. Nguyen, S. Paramesvaran, J. Sturdy, S. Sumowidagdo, R. Wilken, S. Wimpenny

University of California, San Diego, La Jolla, USA

W. Andrews, J.G. Branson, G.B. Cerati, S. Cittolin, D. Evans, F. Golf, A. Holzner, R. Kelley, M. Lebourgeois, J. Letts, I. Macneill, B. Mangano, S. Padhi, C. Palmer, G. Petrucciani, M. Pieri, M. Sani, V. Sharma, S. Simon, E. Sudano, M. Tadel, Y. Tu, A. Vartak, S. Wasserbaech[51], F. Würthwein, A. Yagil, J. Yoo

University of California, Santa Barbara, Santa Barbara, USA

D. Barge, R. Bellan, C. Campagnari, M. D'Alfonso, T. Danielson, K. Flowers, P. Geffert, J. Incandela, C. Justus, P. Kalavase, S.A. Koay, D. Kovalskyi, V. Krutelyov, S. Lowette, N. Mccoll, V. Pavlunin, F. Rebassoo, J. Ribnik, J. Richman, R. Rossin, D. Stuart, W. To, C. West

California Institute of Technology, Pasadena, USA

A. Apresyan, A. Bornheim, Y. Chen, E. Di Marco, J. Duarte, M. Gataullin, Y. Ma, A. Mott, H.B. Newman, C. Rogan, M. Spiropulu[4], V. Timciuc, J. Veverka, R. Wilkinson, Y. Yang, R.Y. Zhu

Carnegie Mellon University, Pittsburgh, USA

B. Akgun, V. Azzolini, R. Carroll, T. Ferguson, Y. Iiyama, D.W. Jang, Y.F. Liu, M. Paulini, H. Vogel, I. Vorobiev

University of Colorado at Boulder, Boulder, USA

J.P. Cumalat, B.R. Drell, C.J. Edelmaier, W.T. Ford, A. Gaz, B. Heyburn, E. Luiggi Lopez, J.G. Smith, K. Stenson, K.A. Ulmer, S.R. Wagner

Cornell University, Ithaca, USA

J. Alexander, A. Chatterjee, N. Eggert, L.K. Gibbons, B. Heltsley, A. Khukhunaishvili, B. Kreis, N. Mirman, G. Nicolas Kaufman, J.R. Patterson, A. Ryd, E. Salvati, W. Sun, W.D. Teo, J. Thom, J. Thompson, J. Tucker, J. Vaughan, Y. Weng, L. Winstrom, P. Wittich

Fairfield University, Fairfield, USA

D. Winn

Fermi National Accelerator Laboratory, Batavia, USA

S. Abdullin, M. Albrow, J. Anderson, L.A.T. Bauerdick, A. Beretvas, J. Berryhill, P.C. Bhat, I. Bloch, K. Burkett, J.N. Butler, V. Chetluru, H.W.K. Cheung, F. Chlebana,

V.D. Elvira, I. Fisk, J. Freeman, Y. Gao, D. Green, O. Gutsche, J. Hanlon, R.M. Harris, J. Hirschauer, B. Hooberman, S. Jindariani, M. Johnson, U. Joshi, B. Kilminster, B. Klima, S. Kunori, S. Kwan, C. Leonidopoulos, J. Linacre, D. Lincoln, R. Lipton, J. Lykken, K. Maeshima, J.M. Marraffino, S. Maruyama, D. Mason, P. McBride, K. Mishra, S. Mrenna, Y. Musienko[52], C. Newman-Holmes, V. O'Dell, O. Prokofyev, E. Sexton-Kennedy, S. Sharma, W.J. Spalding, L. Spiegel, P. Tan, L. Taylor, S. Tkaczyk, N.V. Tran, L. Uplegger, E.W. Vaandering, R. Vidal, J. Whitmore, W. Wu, F. Yang, F. Yumiceva, J.C. Yun

University of Florida, Gainesville, USA

D. Acosta, P. Avery, D. Bourilkov, M. Chen, T. Cheng, S. Das, M. De Gruttola, G.P. Di Giovanni, D. Dobur, A. Drozdetskiy, R.D. Field, M. Fisher, Y. Fu, I.K. Furic, J. Gartner, J. Hugon, B. Kim, J. Konigsberg, A. Korytov, A. Kropivnitskaya, T. Kypreos, J.F. Low, K. Matchev, P. Milenovic[53], G. Mitselmakher, L. Muniz, R. Remington, A. Rinkevicius, P. Sellers, N. Skhirtladze, M. Snowball, J. Yelton, M. Zakaria

Florida International University, Miami, USA

V. Gaultney, S. Hewamanage, L.M. Lebolo, S. Linn, P. Markowitz, G. Martinez, J.L. Rodriguez

Florida State University, Tallahassee, USA

T. Adams, A. Askew, J. Bochenek, J. Chen, B. Diamond, S.V. Gleyzer, J. Haas, S. Hagopian, V. Hagopian, M. Jenkins, K.F. Johnson, H. Prosper, V. Veeraraghavan, M. Weinberg

Florida Institute of Technology, Melbourne, USA

M.M. Baarmand, B. Dorney, M. Hohlmann, H. Kalakhety, I. Vodopiyanov

University of Illinois at Chicago (UIC), Chicago, USA

M.R. Adams, I.M. Anghel, L. Apanasevich, Y. Bai, V.E. Bazterra, R.R. Betts, I. Bucinskaite, J. Callner, R. Cavanaugh, C. Dragoiu, O. Evdokimov, L. Gauthier, C.E. Gerber, D.J. Hofman, S. Khalatyan, F. Lacroix, M. Malek, C. O'Brien, C. Silkworth, D. Strom, N. Varelas

The University of Iowa, Iowa City, USA

U. Akgun, E.A. Albayrak, B. Bilki[54], W. Clarida, F. Duru, S. Griffiths, J.-P. Merlo, H. Mermerkaya[55], A. Mestvirishvili, A. Moeller, J. Nachtman, C.R. Newsom, E. Norbeck, Y. Onel, F. Ozok, S. Sen, E. Tiras, J. Wetzel, T. Yetkin, K. Yi

Johns Hopkins University, Baltimore, USA

B.A. Barnett, B. Blumenfeld, S. Bolognesi, D. Fehling, G. Giurgiu, A.V. Gritsan, Z.J. Guo, G. Hu, P. Maksimovic, S. Rappoccio, M. Swartz, A. Whitbeck

The University of Kansas, Lawrence, USA

P. Baringer, A. Bean, G. Benelli, O. Grachov, R.P. Kenny Iii, M. Murray, D. Noonan, S. Sanders, R. Stringer, G. Tinti, J.S. Wood, V. Zhukova

Kansas State University, Manhattan, USA

A.F. Barfuss, T. Bolton, I. Chakaberia, A. Ivanov, S. Khalil, M. Makouski, Y. Maravin, S. Shrestha, I. Svintradze

Lawrence Livermore National Laboratory, Livermore, USA

J. Gronberg, D. Lange, D. Wright

University of Maryland, College Park, USA

A. Baden, M. Boutemeur, B. Calvert, S.C. Eno, J.A. Gomez, N.J. Hadley, R.G. Kellogg, M. Kirn, T. Kolberg, Y. Lu, M. Marionneau, A.C. Mignerey, K. Pedro, A. Peterman, A. Skuja, J. Temple, M.B. Tonjes, S.C. Tonwar, E. Twedt

Massachusetts Institute of Technology, Cambridge, USA

A. Apyan, G. Bauer, J. Bendavid, W. Busza, E. Butz, I.A. Cali, M. Chan, V. Dutta, G. Gomez Ceballos, M. Goncharov, K.A. Hahn, Y. Kim, M. Klute, K. Krajczar[56], W. Li, P.D. Luckey, T. Ma, S. Nahn, C. Paus, D. Ralph, C. Roland, G. Roland, M. Rudolph, G.S.F. Stephans, F. Stöckli, K. Sumorok, K. Sung, D. Velicanu, E.A. Wenger, R. Wolf, B. Wyslouch, S. Xie, M. Yang, Y. Yilmaz, A.S. Yoon, M. Zanetti

University of Minnesota, Minneapolis, USA

S.I. Cooper, B. Dahmes, A. De Benedetti, G. Franzoni, A. Gude, S.C. Kao, K. Klapoetke, Y. Kubota, J. Mans, N. Pastika, R. Rusack, M. Sasseville, A. Singovsky, N. Tambe, J. Turkewitz

University of Mississippi, University, USA

L.M. Cremaldi, R. Kroeger, L. Perera, R. Rahmat, D.A. Sanders

University of Nebraska-Lincoln, Lincoln, USA

E. Avdeeva, K. Bloom, S. Bose, J. Butt, D.R. Claes, A. Dominguez, M. Eads, J. Keller, I. Kravchenko, J. Lazo-Flores, H. Malbouisson, S. Malik, G.R. Snow

State University of New York at Buffalo, Buffalo, USA

U. Baur, A. Godshalk, I. Iashvili, S. Jain, A. Kharchilava, A. Kumar, S.P. Shipkowski, K. Smith

Northeastern University, Boston, USA

G. Alverson, E. Barberis, D. Baumgartel, M. Chasco, J. Haley, D. Nash, D. Trocino, D. Wood, J. Zhang

Northwestern University, Evanston, USA

A. Anastassov, A. Kubik, N. Mucia, N. Odell, R.A. Ofierzynski, B. Pollack, A. Pozdnyakov, M. Schmitt, S. Stoynev, M. Velasco, S. Won

University of Notre Dame, Notre Dame, USA

L. Antonelli, D. Berry, A. Brinkerhoff, M. Hildreth, C. Jessop, D.J. Karmgard, J. Kolb, K. Lannon, W. Luo, S. Lynch, N. Marinelli, D.M. Morse, T. Pearson, R. Ruchti, J. Slaunwhite, N. Valls, M. Wayne, M. Wolf

The Ohio State University, Columbus, USA

B. Bylsma, L.S. Durkin, C. Hill, R. Hughes, R. Hughes, K. Kotov, T.Y. Ling, D. Puigh, M. Rodenburg, C. Vuosalo, G. Williams, B.L. Winer

Princeton University, Princeton, USA

N. Adam, E. Berry, P. Elmer, D. Gerbaudo, V. Halyo, P. Hebda, J. Hegeman, A. Hunt, P. Jindal, D. Lopes Pegna, P. Lujan, D. Marlow, T. Medvedeva, M. Mooney, J. Olsen, P. Piroué, X. Quan, A. Raval, B. Safdi, H. Saka, D. Stickland, C. Tully, J.S. Werner, A. Zuranski

University of Puerto Rico, Mayaguez, USA

J.G. Acosta, E. Brownson, X.T. Huang, A. Lopez, H. Mendez, S. Oliveros, J.E. Ramirez Vargas, A. Zatserklyaniy

Purdue University, West Lafayette, USA

E. Alagoz, V.E. Barnes, D. Benedetti, G. Bolla, D. Bortoletto, M. De Mattia, A. Everett, Z. Hu, M. Jones, O. Koybasi, M. Kress, A.T. Laasanen, N. Leonardo, V. Maroussov, P. Merkel, D.H. Miller, N. Neumeister, I. Shipsey, D. Silvers, A. Svyatkovskiy, M. Vidal Marono, H.D. Yoo, J. Zablocki, Y. Zheng

Purdue University Calumet, Hammond, USA

S. Guragain, N. Parashar

Rice University, Houston, USA

A. Adair, C. Boulahouache, K.M. Ecklund, F.J.M. Geurts, B.P. Padley, R. Redjimi, J. Roberts, J. Zabel

University of Rochester, Rochester, USA

B. Betchart, A. Bodek, Y.S. Chung, R. Covarelli, P. de Barbaro, R. Demina, Y. Eshaq, A. Garcia-Bellido, P. Goldenzweig, J. Han, A. Harel, D.C. Miner, D. Vishnevskiy, M. Zielinski

The Rockefeller University, New York, USA

A. Bhatti, R. Ciesielski, L. Demortier, K. Goulianos, G. Lungu, S. Malik, C. Mesropian

Rutgers, the State University of New Jersey, Piscataway, USA

S. Arora, A. Barker, J.P. Chou, C. Contreras-Campana, E. Contreras-Campana, D. Duggan, D. Ferencek, Y. Gershtein, R. Gray, E. Halkiadakis, D. Hidas, A. Lath, S. Panwalkar, M. Park, R. Patel, V. Rekovic, J. Robles, K. Rose, S. Salur, S. Schnetzer, C. Seitz, S. Somalwar, R. Stone, S. Thomas

University of Tennessee, Knoxville, USA

G. Cerizza, M. Hollingsworth, S. Spanier, Z.C. Yang, A. York

Texas A&M University, College Station, USA

R. Eusebi, W. Flanagan, J. Gilmore, T. Kamon[57], V. Khotilovich, R. Montalvo, I. Osipenkov, Y. Pakhotin, A. Perloff, J. Roe, A. Safonov, T. Sakuma, S. Sengupta, I. Suarez, A. Tatarinov, D. Toback

Texas Tech University, Lubbock, USA

N. Akchurin, J. Damgov, P.R. Dudero, C. Jeong, K. Kovitanggoon, S.W. Lee, T. Libeiro, Y. Roh, I. Volobouev

Vanderbilt University, Nashville, USA

E. Appelt, A.G. Delannoy, C. Florez, S. Greene, A. Gurrola, W. Johns, C. Johnston, P. Kurt, C. Maguire, A. Melo, M. Sharma, P. Sheldon, B. Snook, S. Tuo, J. Velkovska

University of Virginia, Charlottesville, USA

M.W. Arenton, M. Balazs, S. Boutle, B. Cox, B. Francis, J. Goodell, R. Hirosky, A. Ledovskoy, C. Lin, C. Neu, J. Wood, R. Yohay

Wayne State University, Detroit, USA

S. Gollapinni, R. Harr, P.E. Karchin, C. Kottachchi Kankanamge Don, P. Lamichhane, A. Sakharov

University of Wisconsin, Madison, USA

M. Anderson, M. Bachtis, D. Belknap, L. Borrello, D. Carlsmith, M. Cepeda, S. Dasu, E. Friis, L. Gray, K.S. Grogg, M. Grothe, R. Hall-Wilton, M. Herndon, A. Hervé, P. Klabbers, J. Klukas, A. Lanaro, C. Lazaridis, J. Leonard, R. Loveless, A. Mohapatra, I. Ojalvo, F. Palmonari, G.A. Pierro, I. Ross, A. Savin, W.H. Smith, J. Swanson

†: Deceased
1: Also at Vienna University of Technology, Vienna, Austria
2: Also at National Institute of Chemical Physics and Biophysics, Tallinn, Estonia
3: Also at Universidade Federal do ABC, Santo Andre, Brazil
4: Also at California Institute of Technology, Pasadena, USA
5: Also at CERN, European Organization for Nuclear Research, Geneva, Switzerland
6: Also at Laboratoire Leprince-Ringuet, Ecole Polytechnique, IN2P3-CNRS, Palaiseau, France
7: Also at Suez Canal University, Suez, Egypt
8: Also at Zewail City of Science and Technology, Zewail, Egypt
9: Also at Cairo University, Cairo, Egypt
10: Also at Fayoum University, El-Fayoum, Egypt
11: Also at British University, Cairo, Egypt
12: Now at Ain Shams University, Cairo, Egypt
13: Also at National Centre for Nuclear Research, Swierk, Poland
14: Also at Université de Haute-Alsace, Mulhouse, France
15: Now at Joint Institute for Nuclear Research, Dubna, Russia
16: Also at Moscow State University, Moscow, Russia
17: Also at Brandenburg University of Technology, Cottbus, Germany
18: Also at Institute of Nuclear Research ATOMKI, Debrecen, Hungary
19: Also at Eötvös Loránd University, Budapest, Hungary
20: Also at Tata Institute of Fundamental Research - HECR, Mumbai, India
21: Also at University of Visva-Bharati, Santiniketan, India
22: Also at Sharif University of Technology, Tehran, Iran
23: Also at Isfahan University of Technology, Isfahan, Iran
24: Also at Plasma Physics Research Center, Science and Research Branch, Islamic Azad University, Teheran, Iran

25: Also at Facoltà Ingegneria Università di Roma, Roma, Italy
26: Also at Università della Basilicata, Potenza, Italy
27: Also at Università degli Studi Guglielmo Marconi, Roma, Italy
28: Also at Università degli studi di Siena, Siena, Italy
29: Also at University of Bucharest, Faculty of Physics, Bucuresti-Magurele, Romania
30: Also at Faculty of Physics of University of Belgrade, Belgrade, Serbia
31: Also at University of California, Los Angeles, Los Angeles, USA
32: Also at Scuola Normale e Sezione dell' INFN, Pisa, Italy
33: Also at INFN Sezione di Roma; Università di Roma "La Sapienza", Roma, Italy
34: Also at University of Athens, Athens, Greece
35: Also at Rutherford Appleton Laboratory, Didcot, United Kingdom
36: Also at The University of Kansas, Lawrence, USA
37: Also at Paul Scherrer Institut, Villigen, Switzerland
38: Also at Institute for Theoretical and Experimental Physics, Moscow, Russia
39: Also at Gaziosmanpasa University, Tokat, Turkey
40: Also at Adiyaman University, Adiyaman, Turkey
41: Also at Izmir Institute of Technology, Izmir, Turkey
42: Also at The University of Iowa, Iowa City, USA
43: Also at Mersin University, Mersin, Turkey
44: Also at Ozyegin University, Istanbul, Turkey
45: Also at Kafkas University, Kars, Turkey
46: Also at Suleyman Demirel University, Isparta, Turkey
47: Also at Ege University, Izmir, Turkey
48: Also at School of Physics and Astronomy, University of Southampton, Southampton, United Kingdom
49: Also at INFN Sezione di Perugia; Università di Perugia, Perugia, Italy
50: Also at University of Sydney, Sydney, Australia
51: Also at Utah Valley University, Orem, USA
52: Also at Institute for Nuclear Research, Moscow, Russia
53: Also at University of Belgrade, Faculty of Physics and Vinca Institute of Nuclear Sciences, Belgrade, Serbia
54: Also at Argonne National Laboratory, Argonne, USA
55: Also at Erzincan University, Erzincan, Turkey
56: Also at KFKI Research Institute for Particle and Nuclear Physics, Budapest, Hungary
57: Also at Kyungpook National University, Daegu, Korea